TID, CODE 250

C. A. Wagner, 643

RESONANT SATELLITE GEODESY STUDY

FINAL REPORT

Contract No. NAS5-10469

TRW Report No. 09128.6001-R000

Submitted to

NASA/Goddard Space Flight Center
Greenbelt, Maryland

TRW SYSTEMS GROUP

RESONANT SATELLITE GEODESY STUDY
FINAL REPORT

Contract No. NAS5-10469

TRW Report No. 09128.6001-R000

Submitted to

NASA/Goddard Space Flight Center
Greenbelt, Maryland

by

TRW Systems Group
One Space Park
Redondo Beach, California

Resonant Satellite Geodesy Study

Prepared by: B. C. Douglas

Prepared by: Michael T. Palmiter
M. T. Palmiter

Approved by: G. S. Gedeon
G. S. Gedeon

CONTENTS

SUMMARY OF RESULTS

The investigation of the usefulness of resonant orbits for Geodesy has resulted in the following conclusions:

1. For the determination of high degree and order ($\ell \geq 8$) terms in the geopotential, resonant orbits will be two or three, or more orders of magnitude better (in the sense of smaller standard deviations) than nonresonant orbits as long as (ℓ - m) is less than about five. The exact figures depend upon the orbit in question.

2. Eccentric resonant orbits will yield about two to three times more constants per orbit than circular or nearly circular resonant orbits.

3. Large injection velocity errors, e.g., 20 ft/sec, do not seriously degrade the accuracy of the determination.

4. The problem of separation of the effects of the constants from each other is less critical for resonant orbits than for nonresonant orbits. If observation of multiple satellites is required for separation of constants, small differences in eccentricity are as effective as large differences in inclination.

5. For constants in the range (8, 8) - (15, 15), high inclinations ($i \geq 50^{\circ}$) only are useful.

Having established the importance of resonant orbits in comparison to nonresonant orbits, it is recommended that an error analysis be performed whose goal is the determination of the absolute accuracy with which geopotential constants can be obtained from observation of satellites on eccentric resonant orbits.

1. INTRODUCTION

The purpose of this study has been to obtain quantitative estimates of the relative usefulness of resonant and nonresonant satellite orbits for determination of geopotential constants. The study has established, as seen in the summary, that resonant orbits will be far more useful than nonresonant orbits for determination of many of the high degree and order terms in the geopotential.

The technique of analysis used in this study was to compare covariance matrices of the unknown geopotential constants obtained from simulated observation of both resonant and nonresonant orbits.

This technique presents extreme problems unless great care is taken. The problems arise from the extremely long orbital arcs that must be considered if the high degree terms in the geopotential are to be determined. In this study, orbital arcs of up to 3900 revolutions were considered. The ability to rapidly compute trajectories and partial derivatives of simulated observations with respect to geopotential constants over such long arcs is in itself a formidable requirement, quite apart from the error analysis. For nonresonant orbits, analytic approximations are possible, leading to an efficient means of computation. But for eccentric resonant orbits, no analytic approximation of sufficient accuracy exists. A numerical integration is required. By appropriate choice of dependent variables, a high-speed computation scheme was possible that permitted orbit computation at speeds up to 6000 revolutions/min of IBM 7094 computer time. This is about 400 times faster than conventional techniques. Indeed, this study would have been impossible (except at very greatly increased cost) without the high-speed orbit computation program developed at TRW Systems.

Also considered in this study were the effects of an injection velocity error, data rate, data span, and simultaneous observation of multiple satellites. These cases were studied in terms of the changes in the appropriate covariance matrices.

Finally, graphs have been prepared that permit the analyst to quickly determine which inclinations are optimum for determination of the geopotential constants appropriate to a particular resonant orbit.

2. SATELLITE MOTION THEORY

The phenomenon of resonance in artificial satellite motion manifests itself in the form of extremely large, very long-period along-track oscillations in the motion of the satellite. A detailed discussion of orbital resonance is given in Appendix A of this report.

Mathematically, resonance appears in the form of small divisors in the first order variation of parameters solution to the equations of motion. The small divisors do not imply any particular infinite or wild behavior. Rather, the assumption under which the customary solution is obtained simply breaks down whenever the order (m) subscript of a tesseral harmonic and the mean motion of the satellite (expressed in revs/day) are in the ratio of integers.

To illustrate exactly how this occurs, let us consider the perturbations of the semimajor axis by a tesseral harmonic of degree and order (ℓ, m).

The equation for the variation of the semimajor axis, a, of an orbit is (Reference 17)

$$\frac{da}{dt} = \frac{2}{na} \frac{\partial R}{\partial M} \tag{2.1}$$

where

$$n = \sqrt{\frac{\mu}{a^3}}$$

is the mean motion, M is mean anomaly, and R is the disturbing potential function. The use of equation (2.1) requires that R be expressed in terms of the Kepler elements. Reference 17 gives

$$R_{\ell m} = \frac{\mu a_e^{\ell}}{a^{\ell+1}} J_{\ell m} \sum_{p=o}^{\ell} F_{\ell mp}(i) \cdot \sum_{q=-\infty}^{+\infty} G_{\ell pq}(e) \cdot$$

$$\cdot \begin{cases} \cos \\ \sin \end{cases} \begin{matrix} (\ell - m) \text{ even} \\ (\ell - m) \text{ odd} \end{matrix} [(\ell - 2p)\ \omega + (\ell - 2p + q)\, M + m\,(\Omega - \theta - \lambda_{\ell m})]. \tag{2.2}$$

The quantities a, e, i, Ω, ω, M are the usual Kepler elements. $J_{\ell m}$ and $\lambda_{\ell m}$ are the coefficients associated with a spherical harmonic (ℓ, m). These are related to the $C_{\ell m}$, $S_{\ell m}$ notation by

$$J_{\ell m} = + \left(C_{\ell m}^{\ 2} + S_{\ell m}^{\ 2} \right)^{1/2}$$

$$\lambda_{\ell m} = \frac{1}{m} \tan^{-1} \frac{S_{\ell m}}{C_{\ell m}} \qquad (2.3)$$

The quantity θ is the sidereal time of Greenwich. The inclination function $F_{\ell mp}(i)$ arose when the potential was rotated into the satellite orbit plane. The eccentricity function $G_{\ell pq}(e)$ is a more convenient form of the Hansen Coefficient and is the result of the conversion of the potential from expression in terms of true anomaly to mean anomaly.

Note that Equation (2.2) for $R_{\ell m}$ expresses the potential as a harmonic series in the mean anomaly. For resonance problems, where the resonance is identified by the ratio of the order subscript of a tesseral harmonic and the mean motion of the satellite, this form of the potential is very useful.

Let us now obtain da/dt for a particular harmonic component (p, q) of a particular tesseral harmonic of degree and order (ℓ, m). From Equations (2.1) and (2.2),

$$\left(\frac{da}{dt}\right)_{\ell mpq} = \frac{2}{na} \frac{\mu a_e^{\ \ell}}{a^{\ell+1}} J_{\ell m} F_{\ell mp}(i) G_{\ell pq}(e) \cdot (\ell - 2p + q) \cdot$$

$$\cdot \begin{cases} -\sin \\ +\cos \end{cases} \begin{matrix} (\ell - m)\text{even} \\ (\ell - m)\text{odd} \end{matrix} [(\ell - 2p)\,\omega + (\ell - 2p + q)\,M + m(\Omega - \theta - \lambda_{\ell m})] . \qquad (2.4)$$

Equation (2.4) is seen to have the form

$$\left(\frac{da}{dt}\right)_{\ell mpq} = J_{\ell m} \cdot f(a, e, i)\, g(\omega, M, \Omega, \theta, \lambda_{\ell m}). \qquad (2.5)$$

A first order integration of this equation is possible under the following assumption, viz., that the perturbations due to tesseral harmonics are so small that the effects of tesseral harmonics can be entirely neglected in the calculation of their effects. This is equivalent to regarding tesseral harmonic effects as linear forced oscillations about an intermediary orbit.

Under this assumption $f(a, e, i)$ is considered constant; the changes in $g(\omega, M, \Omega, \theta, \lambda_{\ell m})$ are taken to be only those due to the central force term and the second zonal harmonic. Then separating the variables and integrating Equation (2.4) yields

$$\Delta a_{\ell mpq} = \frac{2}{na}(\ell - 2p + q)\frac{\mu a_e}{a^{\ell+1}} \frac{J_{\ell m} F_{\ell mp}(i) G_{\ell pq}(e)}{[(\ell - 2p)\dot{\omega} + (\ell - 2p + q)\dot{M} + m(\dot{\Omega} - \dot{\theta})]}$$

$$\cdot \begin{Bmatrix} \cos \\ \sin \end{Bmatrix} \begin{matrix} (\ell - m)\,\text{even} \\ (\ell - m)\,\text{odd} \end{matrix} \left[(\ell - 2p)\omega + (\ell - 2p + q)M + m(\Omega - \theta - \lambda_{\ell m})\right]. \qquad (2.6)$$

This solution will be valid as long as the divisor term

$$(\ell - 2p)\dot{\omega} + (\ell - 2p + q)\dot{M} + m(\dot{\Omega} - \dot{\theta}) \qquad (2.7)$$

is not very small or zero.

The meaning of this small or zero divisor is clear. When the divisor is small or zero, the sine or cosine argument of the term in $(da/dt)_{\ell mpq}$ changes slowly or not at all. This implies that the perturbation due to the particular harmonic component (ℓ, m, p, q) will grow steadily and change only over a long period, rather than quickly go through a small cycle. Thus the solution Equation (2.6), breaks down because the assumption of small perturbations is voided.

Considering the divisor, Equation (2.7), since $\dot{\omega}$ and $\dot{\Omega}$ are always small compared to $\dot{M}$ and $\dot{\theta}$, Equation (2.7) will be small or zero when

$$(\ell - 2p + q)\dot{M} \approx m\dot{\theta}$$

or

$$(\ell - 2p + q) = \frac{m}{s} \qquad (2.8)$$

where $\dot{M}$ has been expressed as s revolutions/day ($\dot{\theta}$ = 1 revolution/day). Thus the resonance phenomenon occurs, as stated previously, whenever the order (m) subscript and the orbital frequency of the satellite are in the ratio of integers.

For the nonresonant orbits considered in this study, orbit computation was performed by approximate analytic solutions as Equation (2.6). But for eccentric resonant orbits an analytic solution is not possible except under very special conditions. A numerical solution is required.

The customary numerical solution to the equations of motion of an artificial satellite is a numerical integration technique involving approximation of derivatives by finite differences. Such schemes require the smallest number of derivative evaluations for one prediction interval.

Finite-difference methods are based upon the fact that a smooth function can be approximated by a Taylor series of appropriate order over a given integral. The orbit is integrated by successive applications of this series in a step-wise manner until the boundary is reached. In orbit computation, for a scheme that carries sixth derivatives (differences), about 90 - 100 steps/orbit are required to avoid truncation error in the eighth significant digit. Many steps are required because orbital motion is periodic. The integration scheme is essentially polynomial extrapolation, and a polynomial can fit a periodic function only over a limited range of the independent variable.

Thus, the numerical integration step-size is controlled by the high frequency (short period) contributors to the equations of motion. If dependent variables could be found that had no high frequency variation, large integration steps would result. The polynomial extrapolation would be accurate over a larger range of the independent variable.

For computation of resonant orbits for this study, the mean Kepler elements were chosen as dependent variables. Since the mean elements have no short period variation, large integration steps (up to 80 revolutions were possible. This mean element numerical integration was accomplished by integrating the variations in the Kepler elements for the very long period (i.e., resonant)(ℓ, m, p, q) components of the geopotential.

The nonresonant (ℓ, m, p, q) components were ignored. As will be seen in Section 4, this omission results in a conservative estimate of the usefulness of eccentric resonant orbits for geodesy.

The equations for the variations of the Kepler elements are (Reference 17)

$$\frac{da}{dt} = \frac{2}{na} \frac{\partial R}{\partial M}$$

$$\frac{de}{dt} = \frac{(1 - e^2)}{na^2 e} \frac{\partial R}{\partial M} - \frac{(1 - e^2)^{1/2}}{na^2 e} \frac{\partial R}{\partial \omega}$$

$$\frac{di}{dt} = \frac{\cos i}{na^2 (1 - e^2)^{1/2} \sin i} \frac{\partial R}{\partial M} - \frac{1}{na^2 (1 - e^2)^{1/2} \sin i} \frac{\partial R}{\partial \Omega}$$

$$\frac{d\omega}{dt} = \frac{-\cos i}{na^2 (1 - e^2)^{1/2} \sin i} \frac{\partial R}{\partial i} + \frac{(1 - e^2)^{1/2}}{na^2 e} \frac{\partial R}{\partial e}$$

$$\frac{d\Omega}{dt} = \frac{1}{na^2 (1 - e^2)^{1/2} \sin i} \frac{\partial R}{\partial i}$$

$$\frac{dM}{dt} = \frac{\sqrt{\mu}}{a^{3/2}} - \frac{(1 - e^2)}{na^2 e} \frac{\partial R}{\partial a} - \frac{(1 - e^2)}{na^2 e} \frac{\partial R}{\partial e}$$

Using the potential function, Equation (2.2), and the condition that

$$(\ell - 2p + q) = \frac{m}{s}$$

for resonance, the pertinent (ℓ, m, p, q) - sets can be determined and the equations of motion integrated for these terms.

3. ORBIT SELECTION

The evaluation of resonant versus nonresonant satellite orbits for use in the determination of given constants, $C_{\ell m}$ and $S_{\ell m}$, requires comparison of the best choice of resonant and nonresonant orbits from among those that are useful. For a given value of (ℓ, m), we wish to choose a resonant or nonresonant orbit that will yield the most accurate estimate of $C_{\ell m}$ and $S_{\ell m}$, using the techniques pertinent to analysis of either resonant or nonresonant orbits.

In the study, the comparative value of resonant versus nonresonant orbits was obtained directly from calculated values of the quantities

$$\frac{\sigma^2(\text{unknown})}{\sigma^2(\text{observation})}$$

appearing in the diagonal of the covariance matrix $(A^T A)^{-1}$. The precise inclinations to be used for resonant orbit were obtained indirectly from calculated values of the acceleration of the mean anomaly M due to the effect of the various dominant tesseral harmonics. Such quantities $\ddot{M}_{\ell mpq}$ give an indication of the magnitude of along track displacement to be expected in a given time.

Calculation of the matrix $(A^T A)^{-1}$ is discussed in Section 4. The quantity $\ddot{M}_{\ell mpq}$ due to a single tesseral harmonic $V_{\ell mpq}$ is

$$\ddot{M}_{\ell mpq} = -\frac{3}{2}\,\frac{n}{a}\,\dot{a}_{\ell mpq} + 0(J_{\ell m}\cdot\dot{\psi}_{\ell mpq}) + 0(J^2_{\ell m})$$

where

$$\dot{\psi}_{\ell mpq} = (\ell - 2p)\,\dot{\omega} + (\ell - 2p + q)\,\dot{M} + m(\dot{\Omega} - \dot{\theta})$$

For a resonant orbit $\dot{\psi}_{\ell mpq} = 0$, and

$$\ddot{M}_{\ell mpq} = -3\,\frac{m}{s}\,\mu\,\frac{a_e^{\ell}}{a^{\ell+3}}\,J_{\ell m}\,F_{\ell mp}(i)\;G_{\ell pq}(e)\begin{cases}-\sin\\ \cos\end{cases}\begin{matrix}(\ell-m)\text{ even}\\ \psi_{\ell mpq}\\ (\ell-m)\text{odd}\end{matrix},$$

where s = number of revolutions/day. The various accelerations $\ddot{M}_{\ell mpq}$ will combine in some complicated way for a given orbit and, as the along track librations due to resonance build up, the angles $\psi_{\ell mpq}$ will vary slowly through considerable ranges. Instead of analyzing the resultant effect in detail, a practically impossible task because of the very large number of terms considered, the amplitudes

$$\text{maximum } \ddot{M}_{\ell mpq} = -3 \frac{m}{s} \mu \frac{a_e^{\ell}}{a^{\ell+3}} J_{\ell m} F_{\ell m}(i) G_{\ell pq}(e) \qquad (3.1)$$

were calculated and used as a basis for evaluating the contribution of a single harmonic term $V_{\ell mpq}$ on the observable along track displacement.

The actual magnitude of this along track displacement due to $V_{\ell mpq}$ will vary according to how close the geographical longitude of the node is to one of the stable points of resonant libration. Thus, it might be thought that a suitable choice of λ_o, the initial mean longitude of the ascending node must be made to insure that there will be strong observable librational effects from each of the tesseral harmonics under investigation. However, it has been shown (Appendix A) that the longitudes of the stable points of a tesseral harmonic component $V_{\ell mpq}$ move along the equator at a rate $\frac{q}{m}\dot{\omega}$. This, together with the fact that resonant tesseral harmonics occur in pairs $V_{\ell mpq}$, $V_{\ell mp'(-q)}$ with stable points moving in opposite directions at the rate $\frac{q}{m}\dot{\omega}$, obviates the need to place λ_o at any best value. The changes in ω due to the second zonal harmonic insure that over a period of a few months, strong perturbations due to the critical terms will occur. The secular effects of the second zonal harmonic were, of course, included in this study.

More important than any choice of λ_o from the standpoint of mission and vehicle design is the choice of semimajor axis, eccentricity, and inclination of the resonant orbit. The value of the semimajor axis, a, is determined by the fact that the orbit be resonant, or nearly so, with one or more terms of the geopotential. However, we are free to choose the value of the eccentricity in such a way as to maximize observable resonance effects, so long as e does not exceed

$$e_{max} = 1 - \frac{a_e + h_{min}}{a},$$

where h_{min} = minimum possible altitude of perigee of a drag-free orbit. Approximate values for the resonant semimajor axis, a_{res}, and for e_{max} (with $h_{min} = a_e/8$ for $s \leq 14$ and $h_{min} = 0.08\,a_e$ for $s = 15$) are given in Table 3-1. Exact values for a_{res} must be obtained from the condition that the orbit have a repeating ground track.

Elementary computer programs were devised to calculate tables of the functions $F_{\ell mp}(e)$ and $G_{\ell pq}(e)$. It was found that in all cases except $s = 1$ the functions $|G_{\ell pq}(e)|$ occurring as factors in the expression for $|\ddot{M}_{\ell mpq}|$ are monotone increasing functions of e in the interval $0 \leq e \leq e_{max}$. Therefore, the best choice of eccentricity for a resonant orbit, the choice which will in fact maximize all resonant $\ddot{M}_{\ell mpq}$, will be $e = e_{max}$. Even in the case $s = 1$ most of the $G_{\ell pq}(e)$ are monotone, and those that are not are no more than an order of magnitude smaller at $e = e_{max}$ than at their maximum value throughout $0 \leq e \leq e_{max}$.

The reasons for choosing $e = e_{max}$ go further: although resonant terms $V_{\ell mpq}$ for which $q = 0$ will have their effect even if $e = 0$, the effect of terms for which $q \neq 0$ will vanish as e becomes smaller. Since it is desirable to obtain information on as many resonant terms of the geopotential as possible from one orbit, larger values of e are preferred.

The effect of inclination is considered next. Figures 3-1 to 3-21 are semilogarithmic graphs of the maximum value of $|\ddot{M}_{\ell mpq}|$ for the dominant resonant $V_{\ell mpq}$'s for $s = 2$ to $s = 15$. Eccentricity in each case was fixed at $e = e_{max}$ and $|\ddot{M}_{\ell mpq}|_{max}$ is displayed as a function of inclination for $0^\circ \leq i \leq 90^\circ$. Values of ℓmpq were included for which

$$\ell \leq 15 \text{ and } \ell \leq m + 5$$

$$m = s,\ 2s$$

$$q = -1,\ 0,\ +1.$$

It is shown in Appendix A that terms for $|q| > 1$ have only small effect.

Known values of the constants up to (12, 12) as reported by Kaula (Reference 18) were used in Equation 3.1. For values of the constants not listed in Kaula, the expression $10^{-6}/\ell^2$ was used for the normalized $\overline{C}_{\ell m}$, $\overline{S}_{\ell m}$ quantities. Values of the constants calculated in this way agree well with the known values and should yield a useful estimate of $|\ddot{M}_{\ell mpq}|_{max}$.

Table 3-1. Approximate Value for the Semimajor Axis

S (REVS/DAY)	a_{res} (a_e; APPROX.)	e_{max} ($=1 - \frac{1.125}{a_{res}}$)
1	6.6	.8
2	4.16	.73
3	3.18	.65
4	2.62	.57
5	2.26	.50
6	2.00	.44
7	1.80	.37
8	1.65	.32
9	1.52	.26
10	1.42	.21
11	1.33	.15
12	1.25	.10
13	1.20	.06
14	1.13	.01
15*	1.08*	0*

*THE VALUE OF e_{max} FOR s = 15 IS BASED ON $h_{min} = 0.08\ a_e$; THE SATELLITE WOULD HAVE TO BE VERY DENSE TO BE CONSIDERED DRAG FREE.

For the cases of special interest in this study ($s \geq 8$), it can be seen from inspection of the graphs that resonant effects are negligibly small for the lower values of inclination (say, $i \leq 40^{\circ}$). In fact, $40^{\circ} \leq i \leq 80^{\circ}$ would seem to be about the best values for inclination, bringing strong effects from virtually all resonant terms in all cases with $s \geq 8$. The exact choice of i depends on which specific coefficients $C_{\ell m}$ and $S_{\ell m}$ are sought.

The effect of choice of eccentricity must be mentioned again. As the value of s increases, the value of e_{max} decreases, becoming 0.01 for s = 14; for s = 15, we have had to lower h_{min} to 0.08 earth radii and set e = o, requiring a dense satellite to overcome drag. Because of the very small values of e_{max} resulting from the higher values of s, the factor $G_{\ell pq}(e)$ in the expression for $\ddot{M}_{\ell mpq}$ will become smaller (vanishing small for terms in which $q \neq o$). This lessening of detectable effects for high s can be observed in the graphs of $\ddot{M}_{\ell mpq}$ for s = 13, 14, and 15 and is reflected also in decreasing utility of such orbits, as reported in the results (Section 5).

The best choice of orbit elements for a geodetic satellite in a nonresonant orbit is somewhat simpler than in the resonant case. In the case of nonresonant orbits, there is no restriction on the orbit elements other than to place the orbit outside the atmosphere. The aim is to choose elements that will place the orbit at all times where it will be the most strongly perturbed by irregularities of the geopotential. The orbit chosen for the nonresonant cases was a circular orbit placed at the lowest possible altitude at which drag effects may be neglected. This leaves the choice of inclination. The resonant (ℓ, m, p, q) sets of the geopotential were regarded to be a random sample of terms $V_{\ell mpq}$ (terms with q = o will be the only important ones because of the choice e = o). The correctness of this assumption was verified by calculation of covariance matrices for several inclinations.

The resonant orbit selection graphs, Figures 3-1 through 3-21 were prepared with a fixed value of eccentricity in every case. However, this does not negate their use for orbits of other eccentricities. The graphs show plots of the absolute value of the maximum values of the acceleration of the mean anomaly. Since the inclination function has zeros and changes

of sign (not shown on the graphs), the semi-log plots show regions of very sharp decline and rise in the absolute value of $\dot{M}$. These areas to be avoided are solely due to the effect of inclination and thus will be there regardless of eccentricity. Suitable inclinations can be chosen from these graphs for orbits of any eccentricity.

The effect of eccentricity on Figures 3-1 to 3-21 will be to change the values of the $|\dot{M}|$ indicated, particularly for those cases with $q \neq o$. Such cases would be entirely eliminated if eccentricity were made zero.

To use the graphs definitively for other eccentricities, the following procedure can be followed.

First, choose inclination. Then, multiply the $|\dot{M}|$ figures by

$$\frac{G_{\ell pq}\ (\text{new eccentricity})}{G_{\ell pq}\ (\text{eccentricity of graph})}$$

This will divide out the graph value of the eccentricity function and replace it with the new one and will yield then the correct relative amplitudes of the $|\dot{M}|$ for the chosen inclination.

An important result of this study was the discovery that terms with $m/s = 2$ are very important for eccentric resonant orbits. This is strictly due to the eccentricity and hence greatly enhances the importance of moderate and highly eccentric orbits for geodesy. Terms for $m/s = 2$ up to $m = 14$ have been included.

Finally, a significant effect is to be noted from the graphs between the cases $s = 12$ and $s = 13$. Because of decreasing permissible eccentricity, beginning with $s = 13$, the terms with $|q| \neq o$ begin rapidly fading in importance compared to the $q = o$ term. This occurs because as previously noted, the eccentricity function $G_{\ell pq}(e)$ is proportional to $e^{|q|}$ for low e and hence goes to zero for zero e. This fact substantially reduces the usefulness of resonant orbits for $s > 12$ revolutions/day.

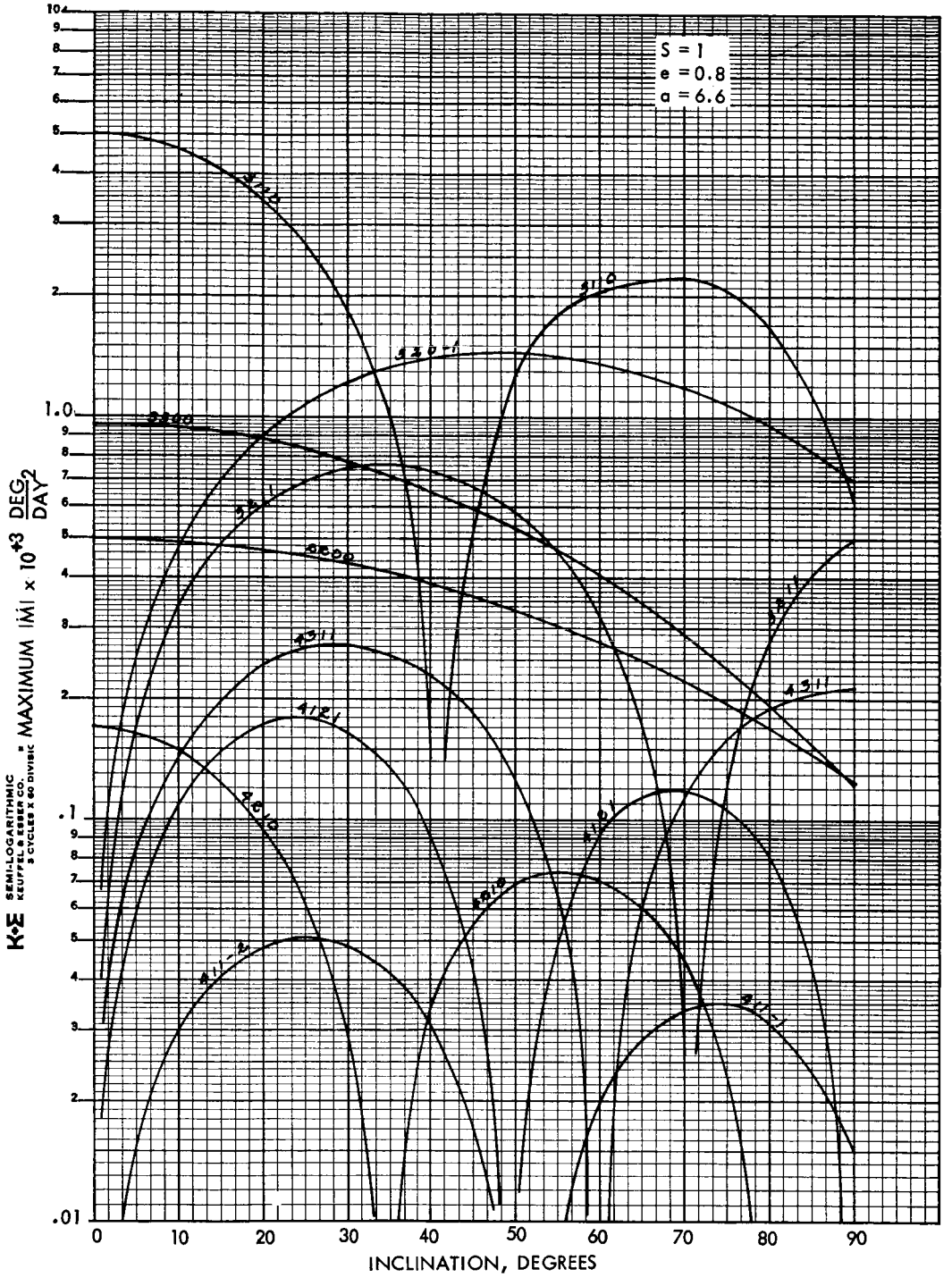
S = 1
e = 0.8
a = 6.6
MAXIMUM |Ṁ| x 10^-3 DEG/DAY^2
INCLINATION, DEGREES
0
10
20
30
40
50
60
70
80
90
.01
.1
1.0
K+E SEMI-LOGARITHMIC
KEUFFEL & ESSER CO.
5 CYCLES X 90 DIVISIC

Figure 3-1

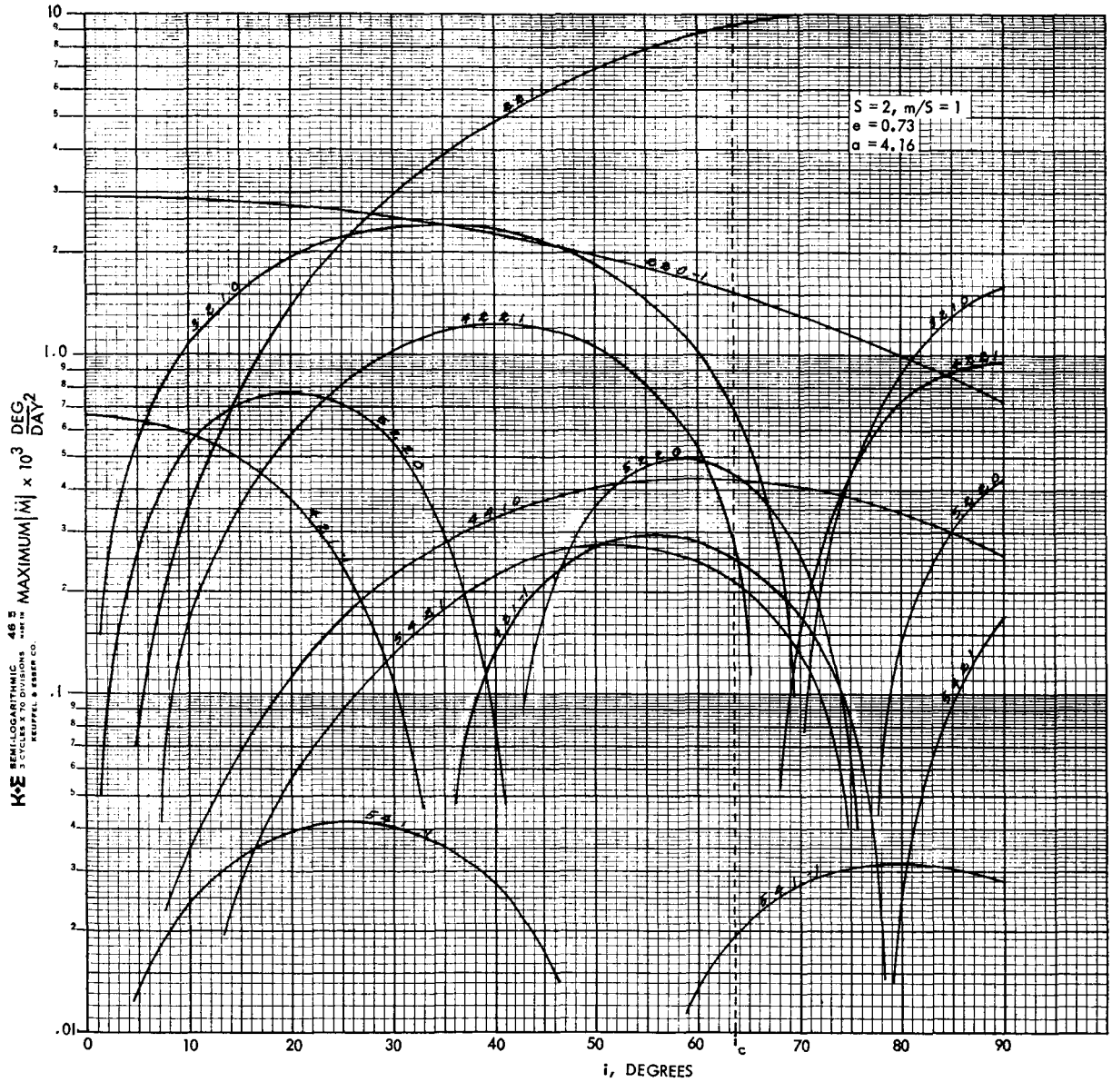
S = 2, m/S = 1
e = 0.73
a = 4.16
MAXIMUM |Ω̇| x 10^3 DEG/DAY^2
i, DEGREES
i_c
10
1.0
.1
.01
0
10
20
30
40
50
60
70
80
90

Figure 3-2

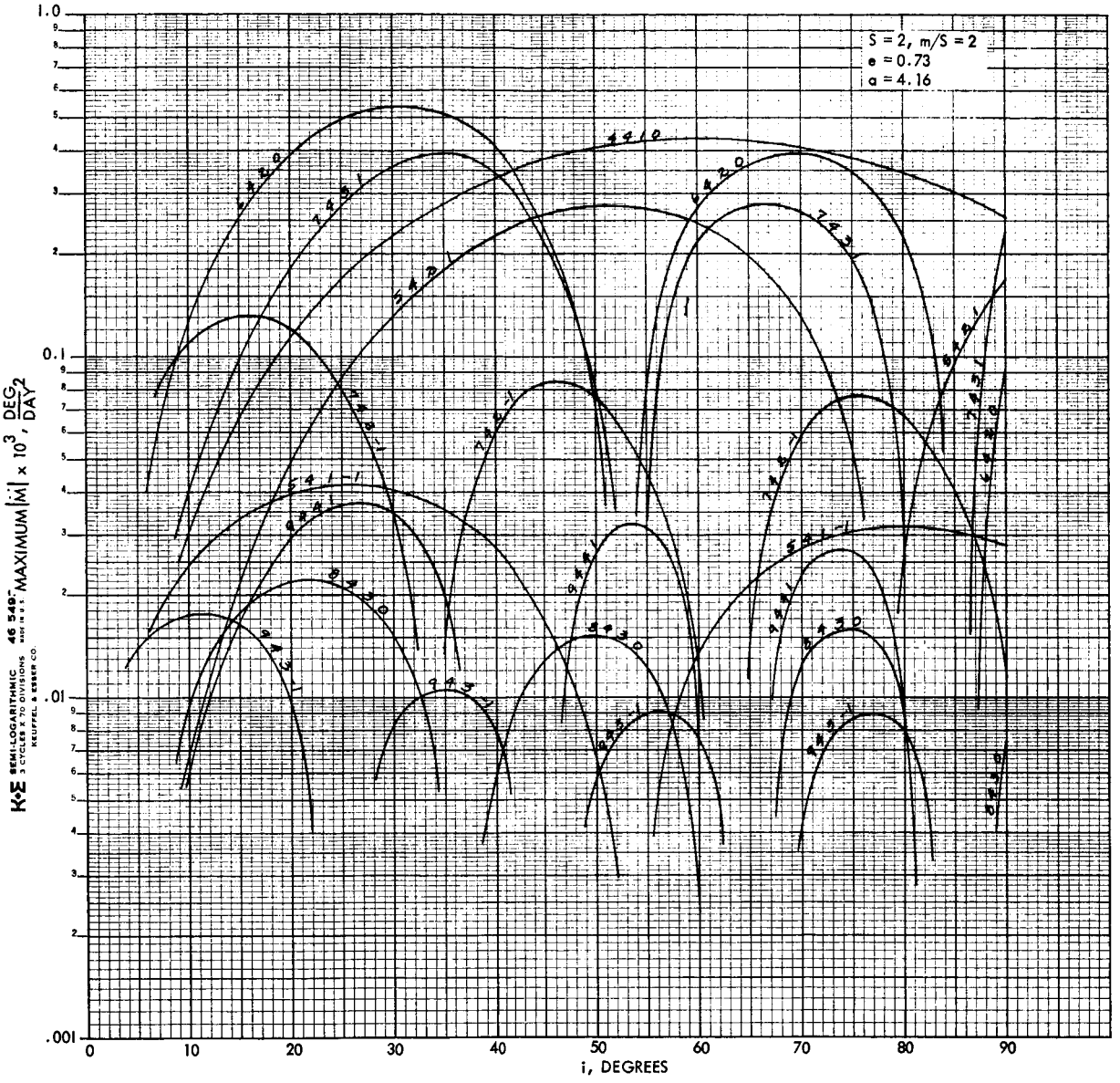
S = 2, m/S = 2
e = 0.73
a = 4.16
MAXIMUM |i| x 10^3, DEG/DAY^2
i, DEGREES
1.0
0.1
.01
.001
0
10
20
30
40
50
60
70
80
90

Figure 3-3

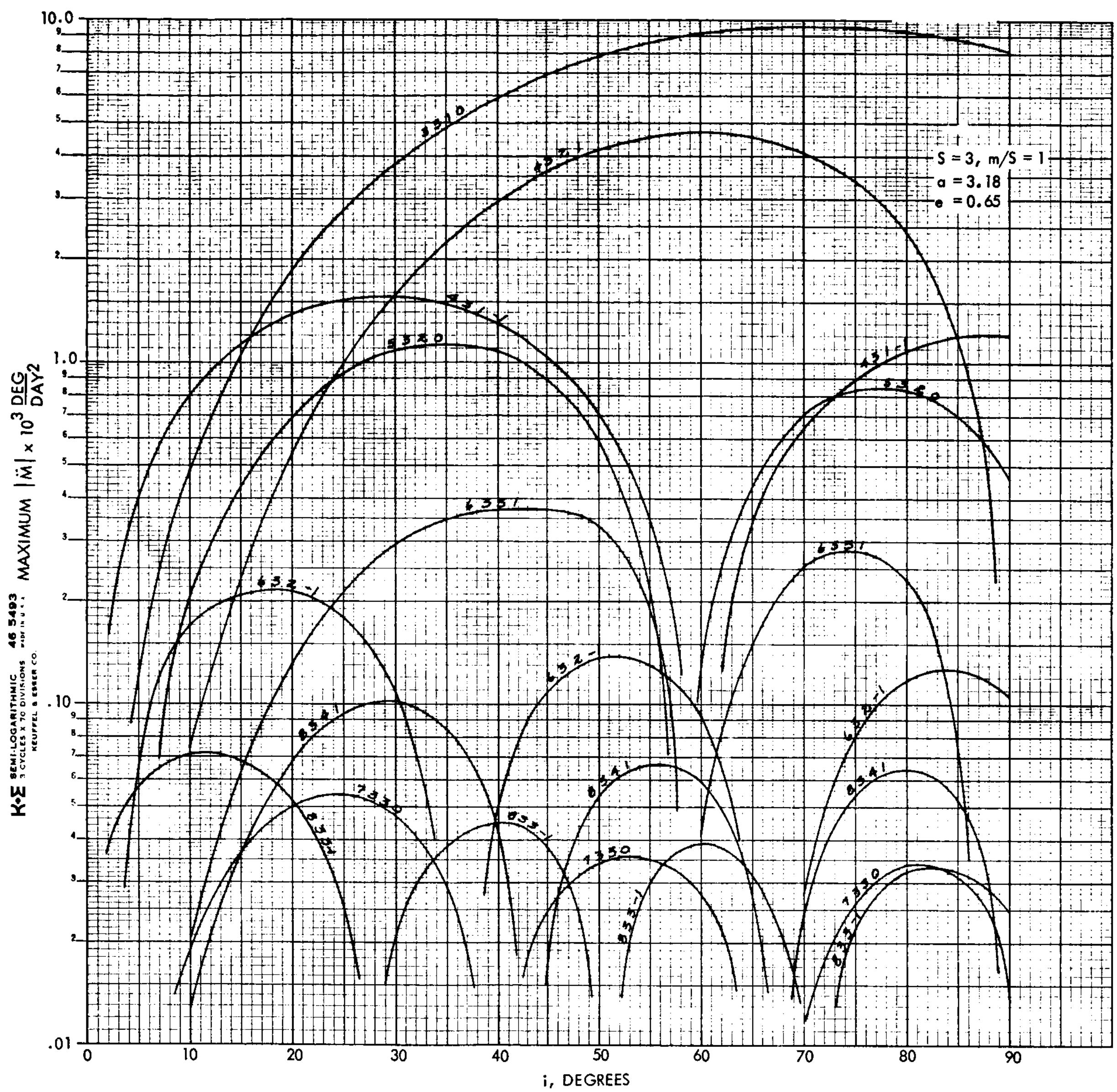
S = 3, m/S = 1
a = 3.18
e = 0.65
MAXIMUM |M̈| x 10^3 DEG/DAY2
i, DEGREES
10.0
1.0
.10
.01
0
10
20
30
40
50
60
70
80
90
K+E SEMI-LOGARITHMIC 46 5493
3 CYCLES X 70 DIVISIONS
KEUFFEL & ESSER CO.

Figure 3-4

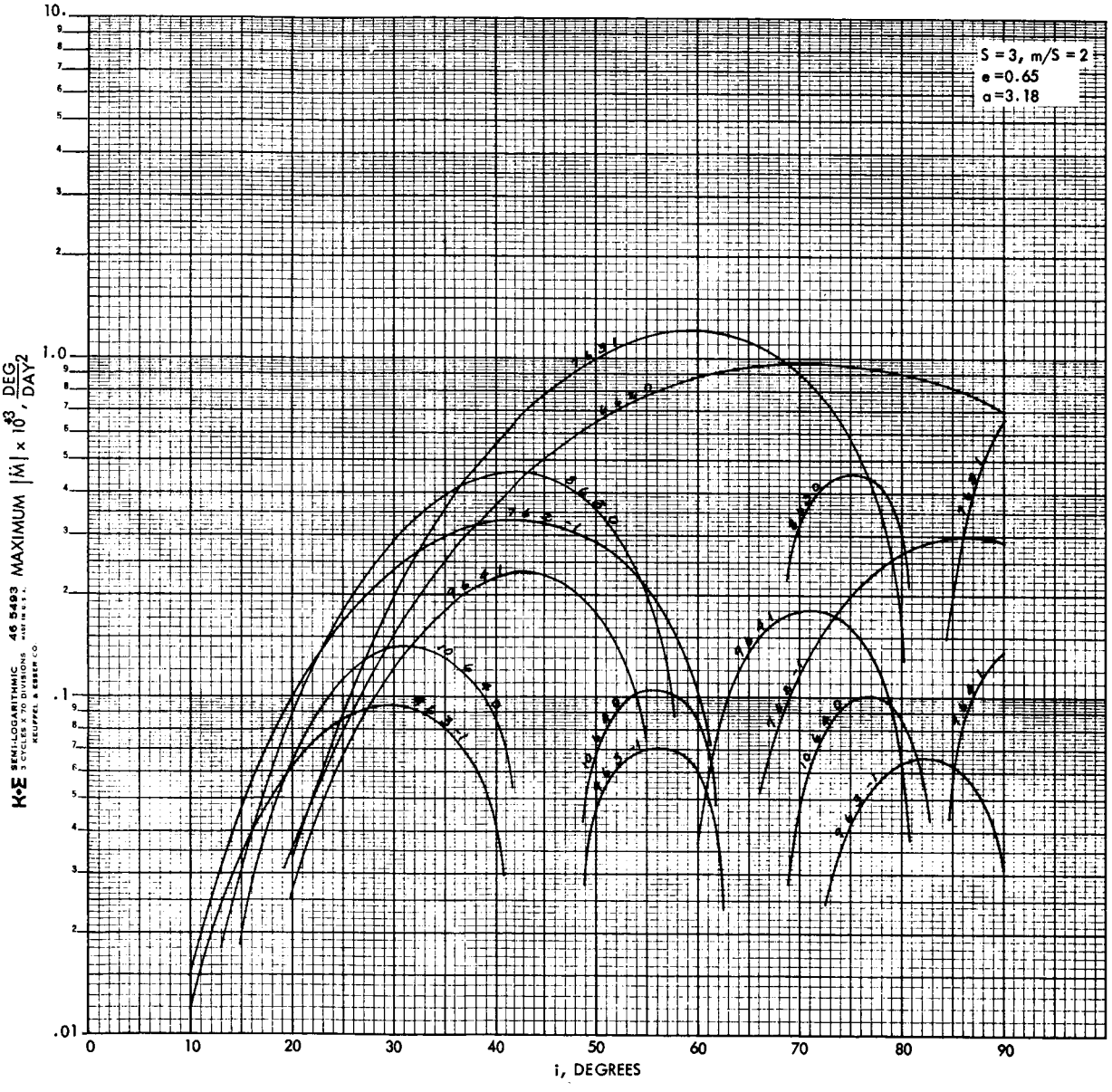
S = 3, m/S = 2
e = 0.65
a = 3.18
MAXIMUM |Ṁ| x 10^3, DEG/DAY^2
i, DEGREES
10.
1.0
.1
.01
0
10
20
30
40
50
60
70
80
90

Figure 3-5

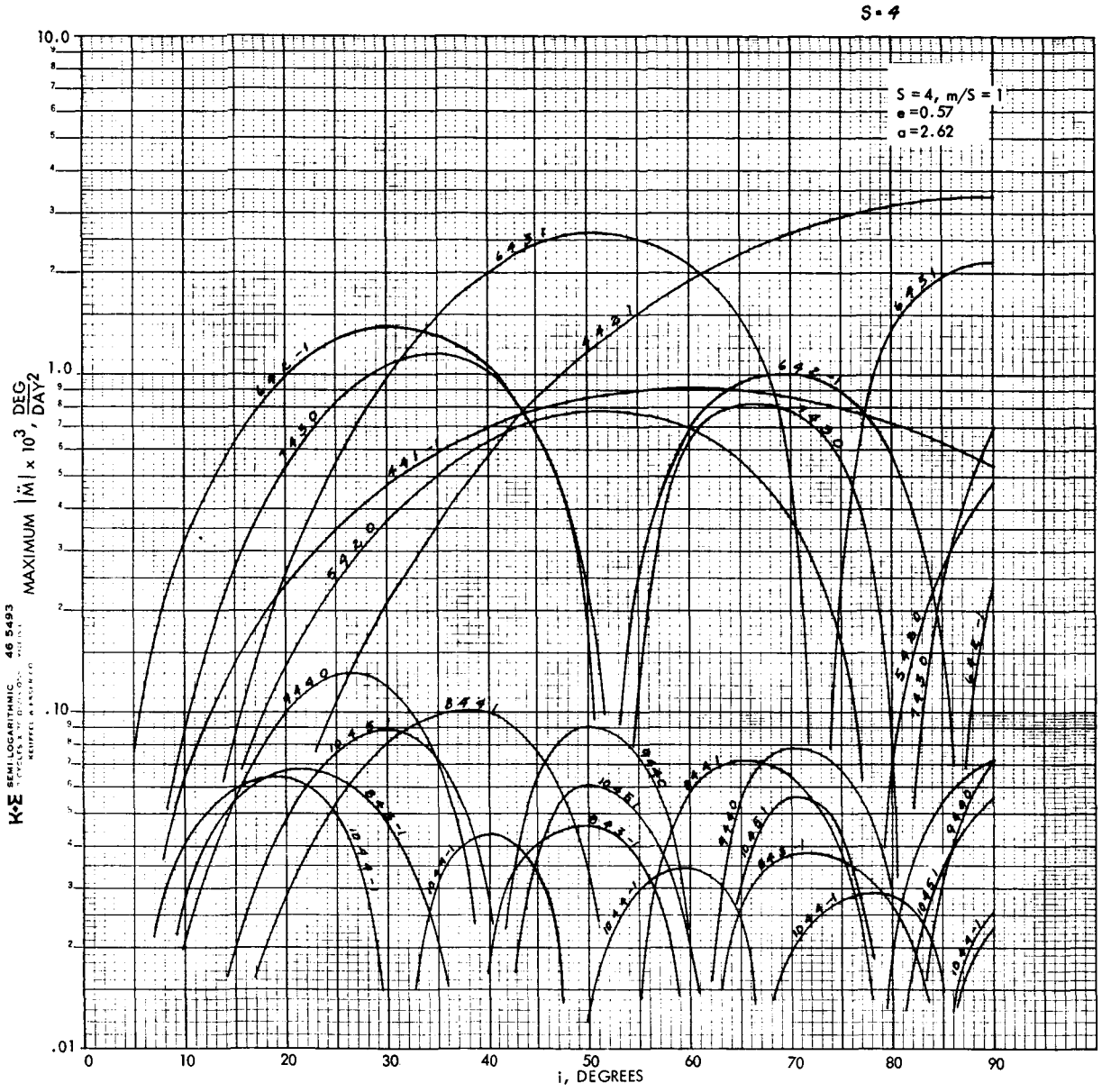
S = 4
S = 4, m/S = 1
e = 0.57
a = 2.62
MAXIMUM |M̈| x 10³, DEG/DAY²
i, DEGREES
10.0
1.0
.10
.01
0
10
20
30
40
50
60
70
80
90

Figure 3-6

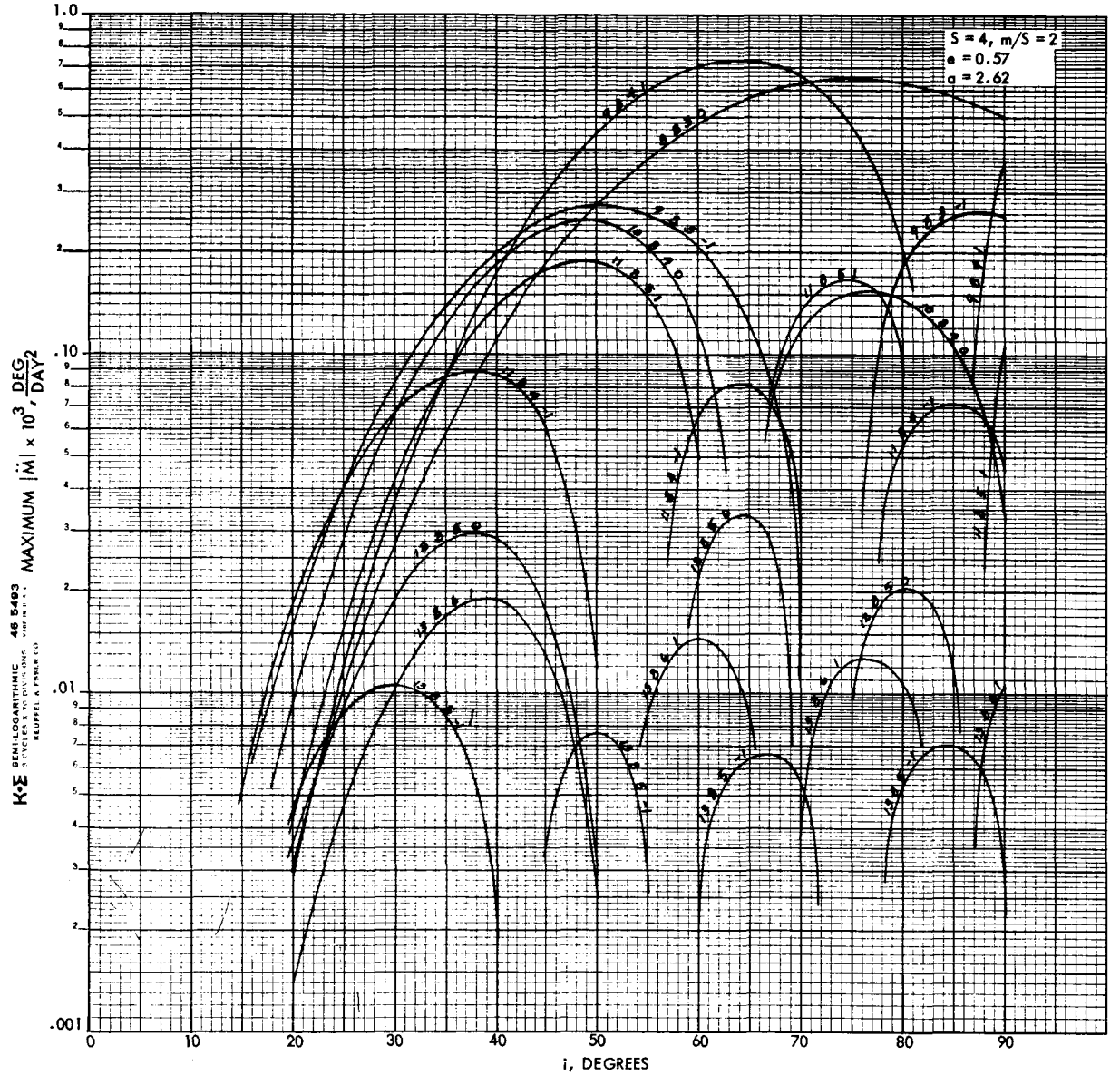
S = 4, m/S = 2
e = 0.57
a = 2.62
MAXIMUM |M̈| x 10³, DEG/DAY²
i, DEGREES
1.0
.10
.01
.001
0
10
20
30
40
50
60
70
80
90
K•E SEMI-LOGARITHMIC 46 5493
KEUFFEL & ESSER CO

Figure 3-7

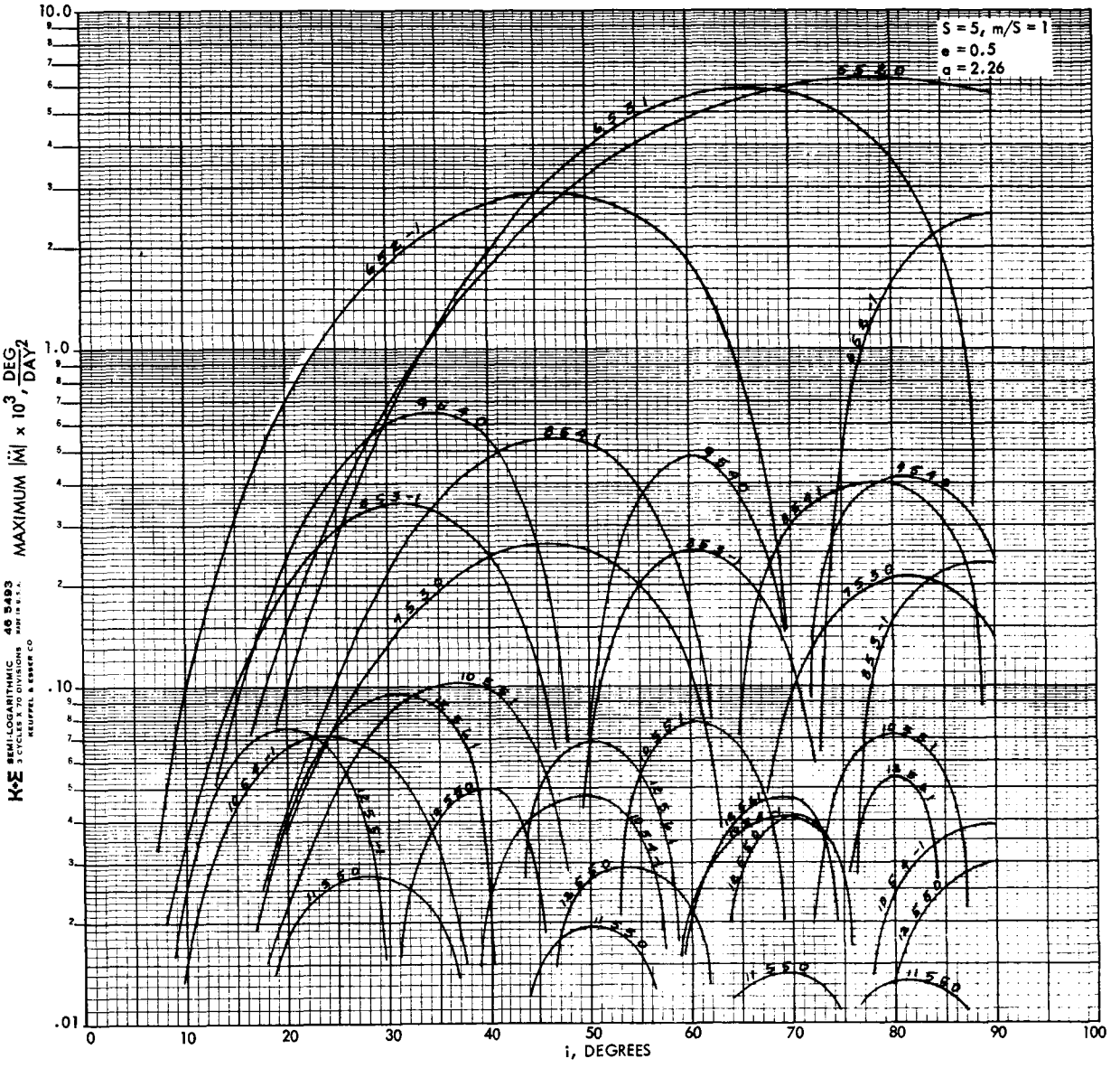
S = 5, m/S = 1
e = 0.5
a = 2.26
MAXIMUM |M̈| x 10³, DEG/DAY²
i, DEGREES
10.0
1.0
.10
.01
0
10
20
30
40
50
60
70
80
90
100

Figure 3-8

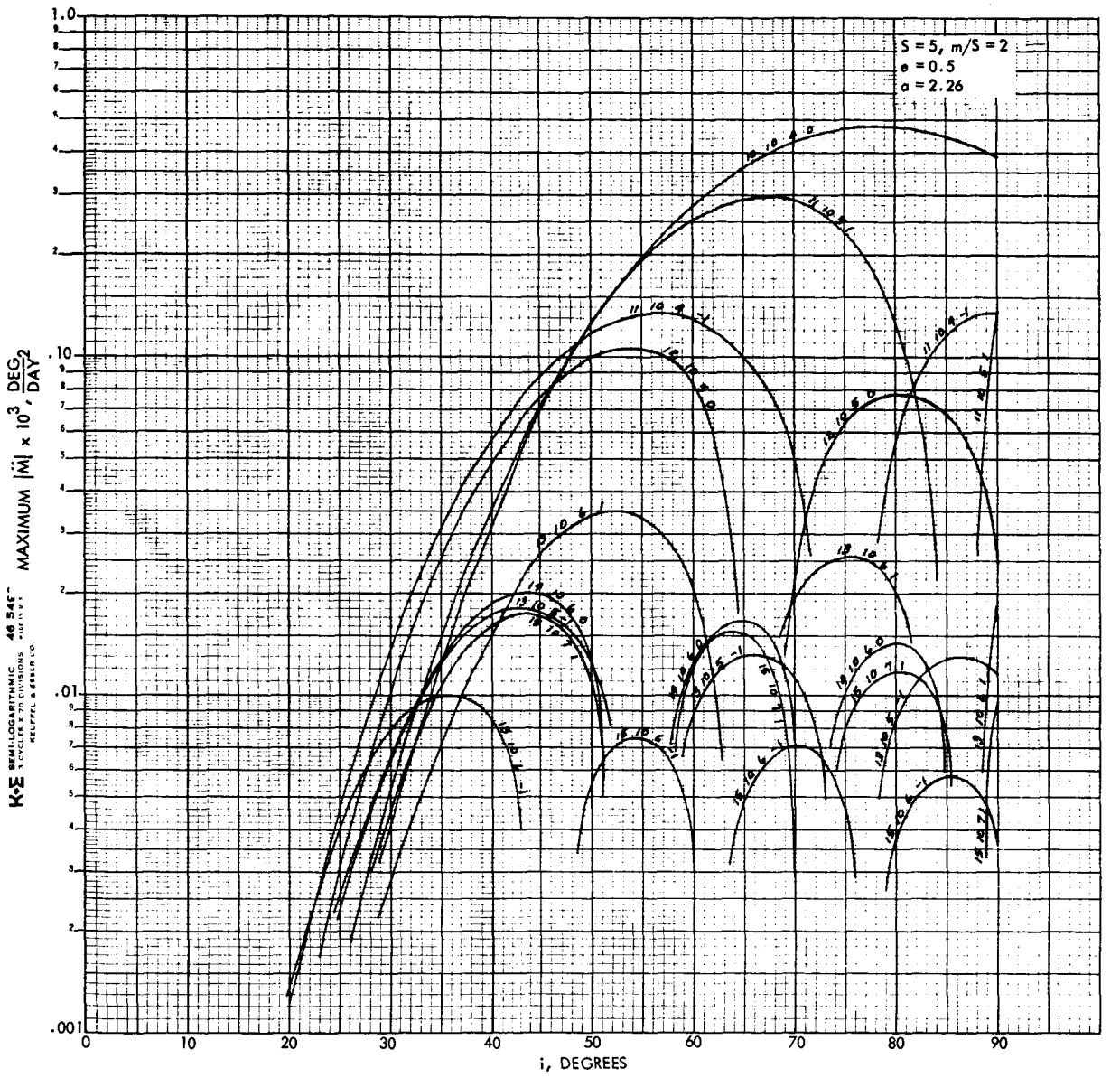
S = 5, m/S = 2
e = 0.5
a = 2.26
MAXIMUM |M̈| x 10³, DEG/DAY²
i, DEGREES
1.0
.10
.01
.001
0
10
20
30
40
50
60
70
80
90

Figure 3-9

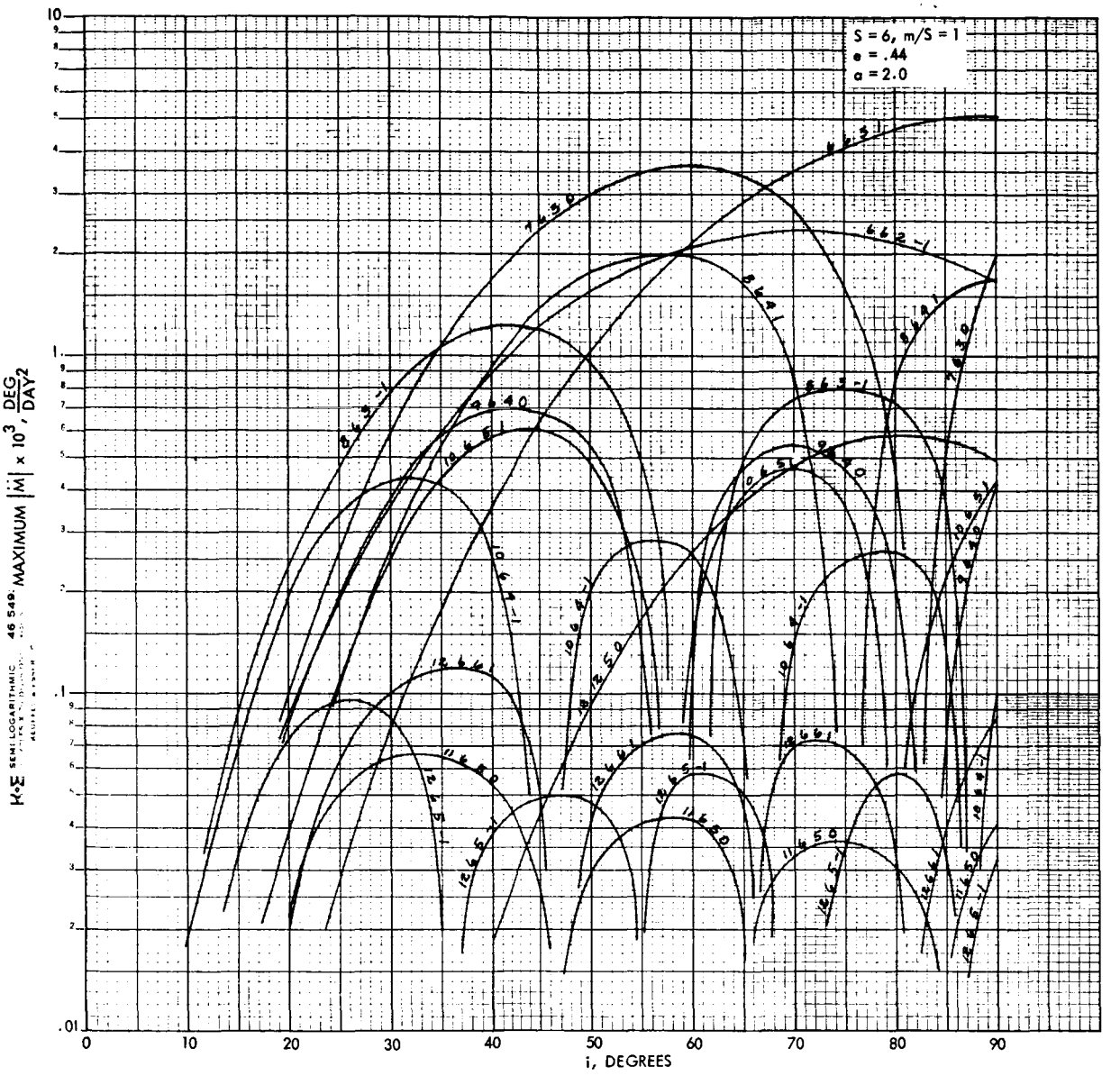
S = 6, m/S = 1
e = .44
a = 2.0
MAXIMUM |M̈| x 10³, DEG/DAY²
i, DEGREES
0
10
20
30
40
50
60
70
80
90
10
.01

Figure 3-10

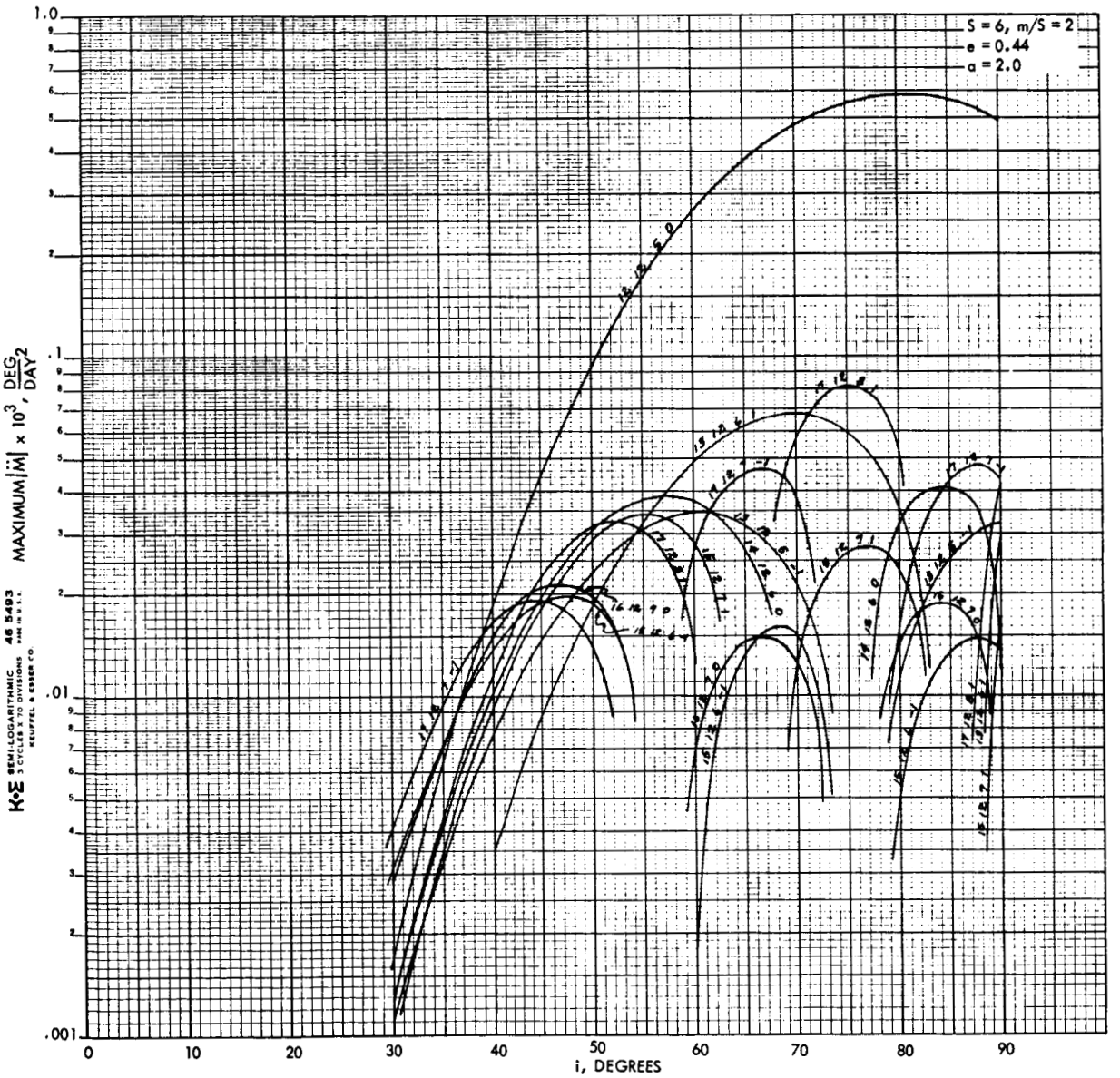
S = 6, m/S = 2
e = 0.44
a = 2.0
MAXIMUM |i| x 10^3, DEG/DAY^2
i, DEGREES
1.0
.1
.01
.001
0
10
20
30
40
50
60
70
80
90
K+E SEMI-LOGARITHMIC 46 5493
3 CYCLES X 70 DIVISIONS
KEUFFEL & ESSER CO.

Figure 3-11.

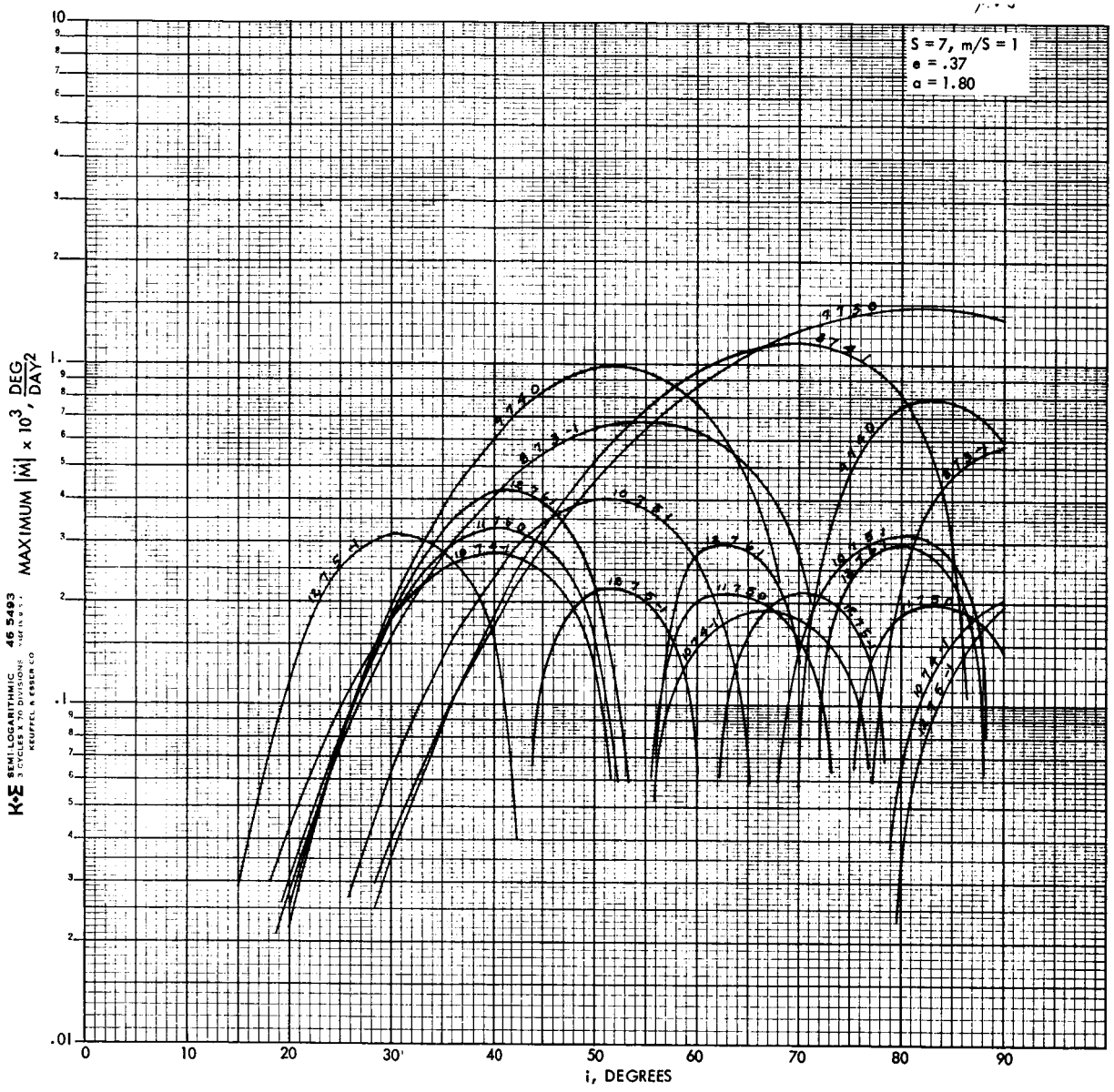
S = 7, m/S = 1
e = .37
a = 1.80
MAXIMUM |M̈| x 10³, DEG/DAY2
i, DEGREES
0
10
20
30
40
50
60
70
80
90
10
1.
.1
.01
K&E SEMI-LOGARITHMIC 46 5493
KEUFFEL & ESSER CO

Figure 3-12

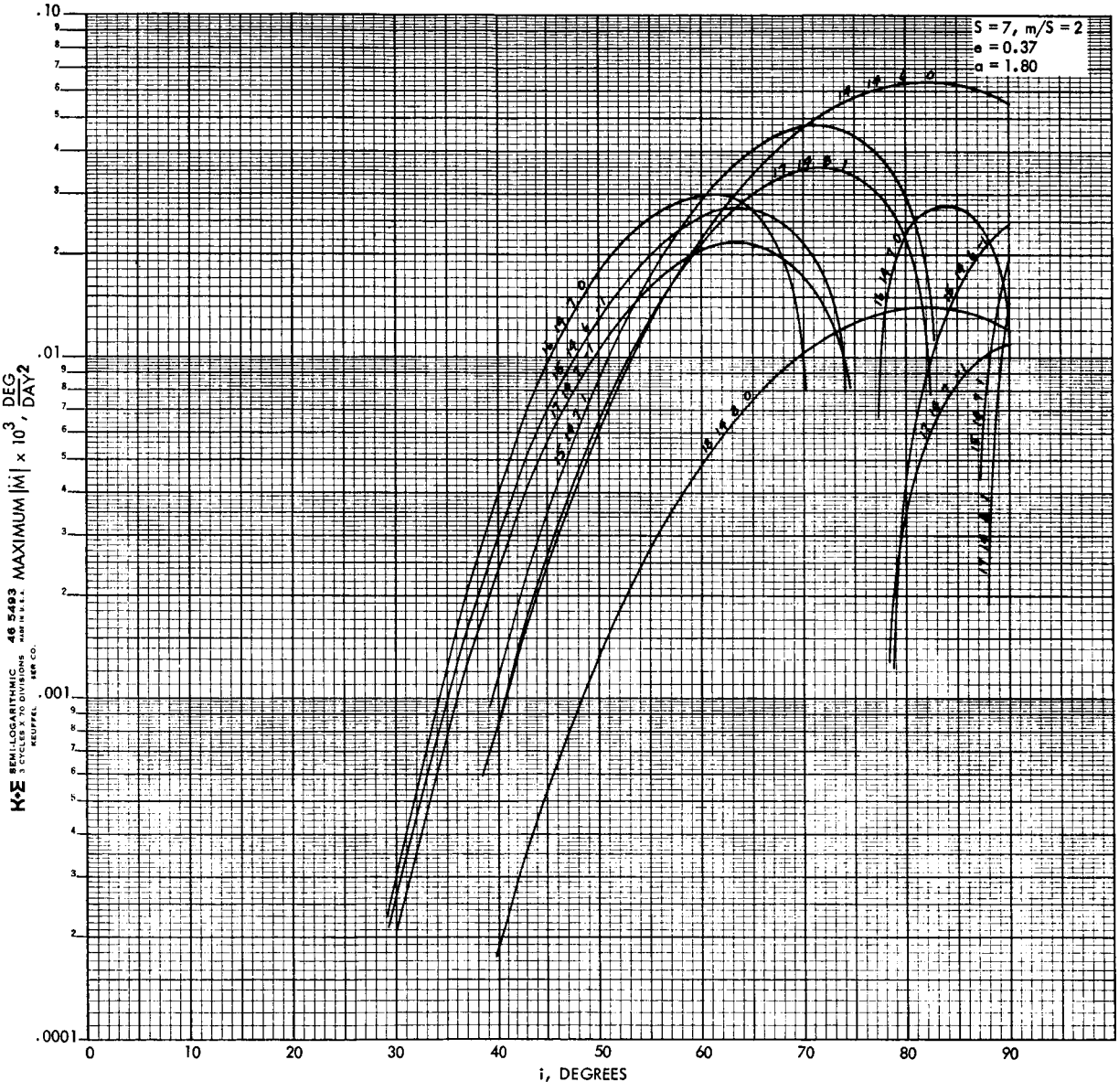
S = 7, m/S = 2
e = 0.37
a = 1.80
MAXIMUM |Ṁ| x 10^3, DEG/DAY^2
i, DEGREES
.10
.01
.001
.0001
0
10
20
30
40
50
60
70
80
90

Figure 3-13

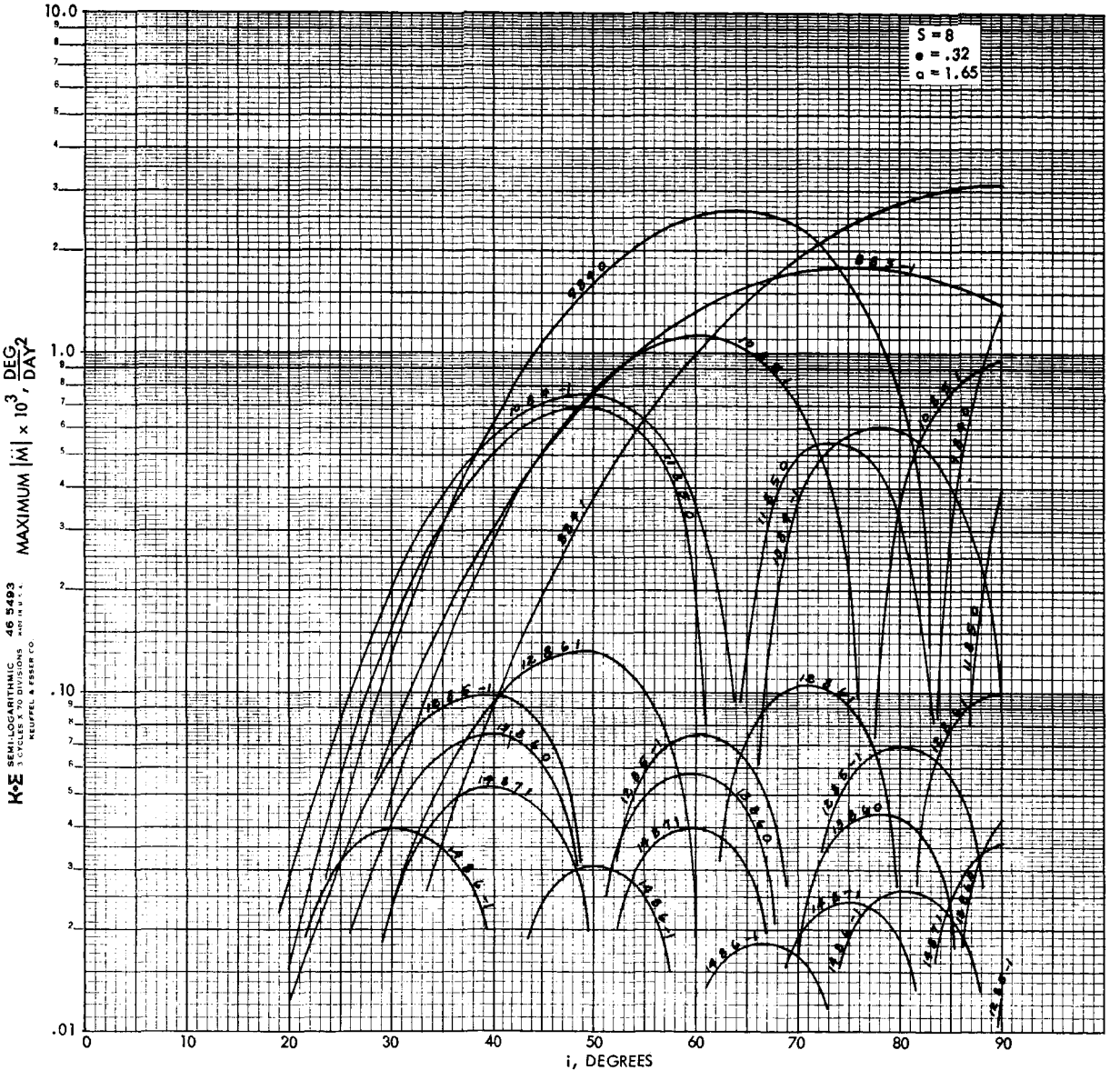
S = 8
e = .32
a = 1.65
MAXIMUM |M| x 10^3, DEG/DAY^2
i, DEGREES
10.0
1.0
.10
.01
0
10
20
30
40
50
60
70
80
90
K+E SEMI-LOGARITHMIC
46 5493
3 CYCLES X 70 DIVISIONS
KEUFFEL & ESSER CO.

Figure 3-14

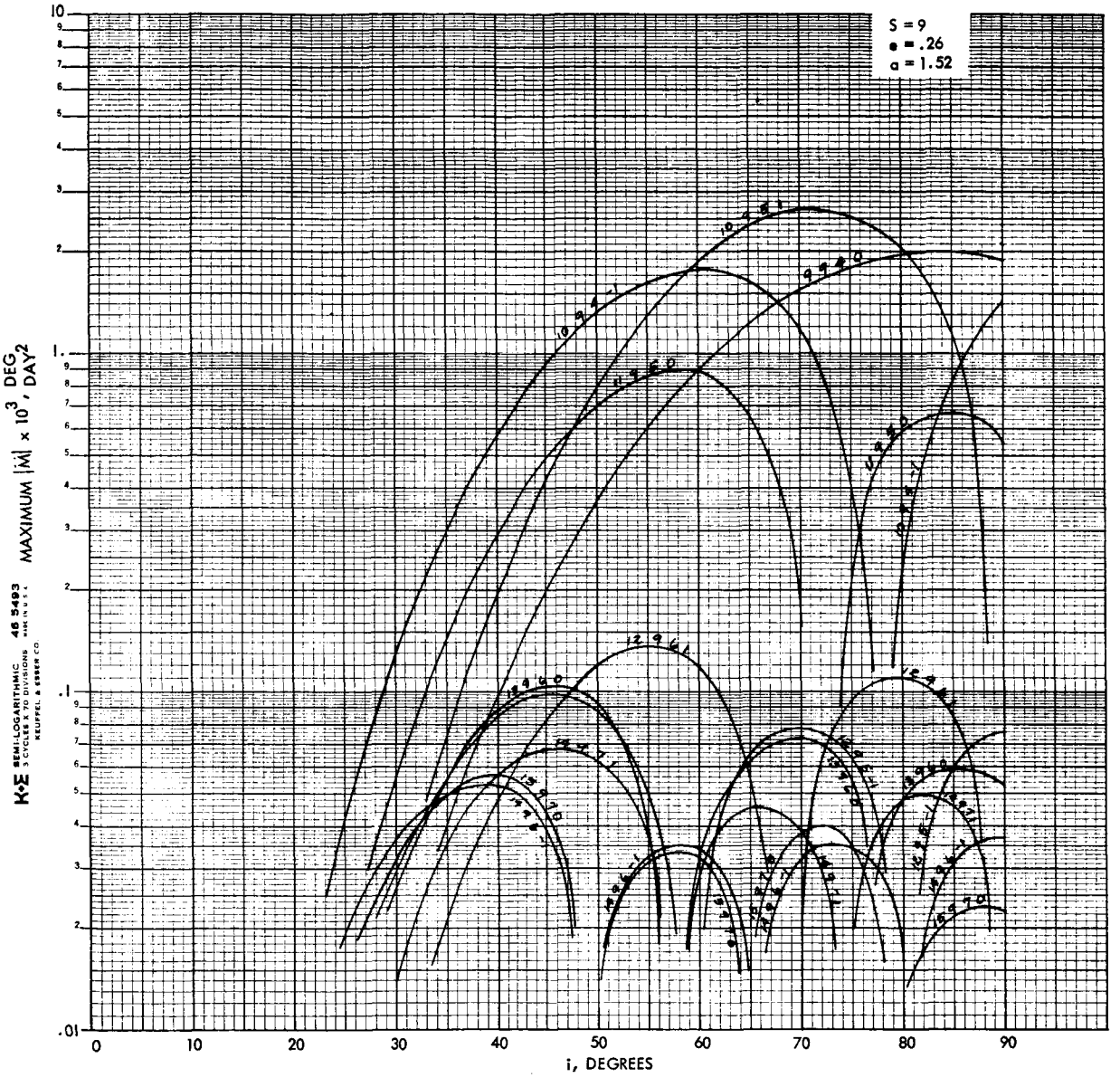
S = 9
e = .26
a = 1.52
MAXIMUM |di| x 10^3, DEG/DAY^2
i, DEGREES
10
1.
.1
.01
0
10
20
30
40
50
60
70
80
90
K+E SEMI-LOGARITHMIC 46 5493
3 CYCLES X 70 DIVISIONS
KEUFFEL & ESSER CO.

Figure 3-15

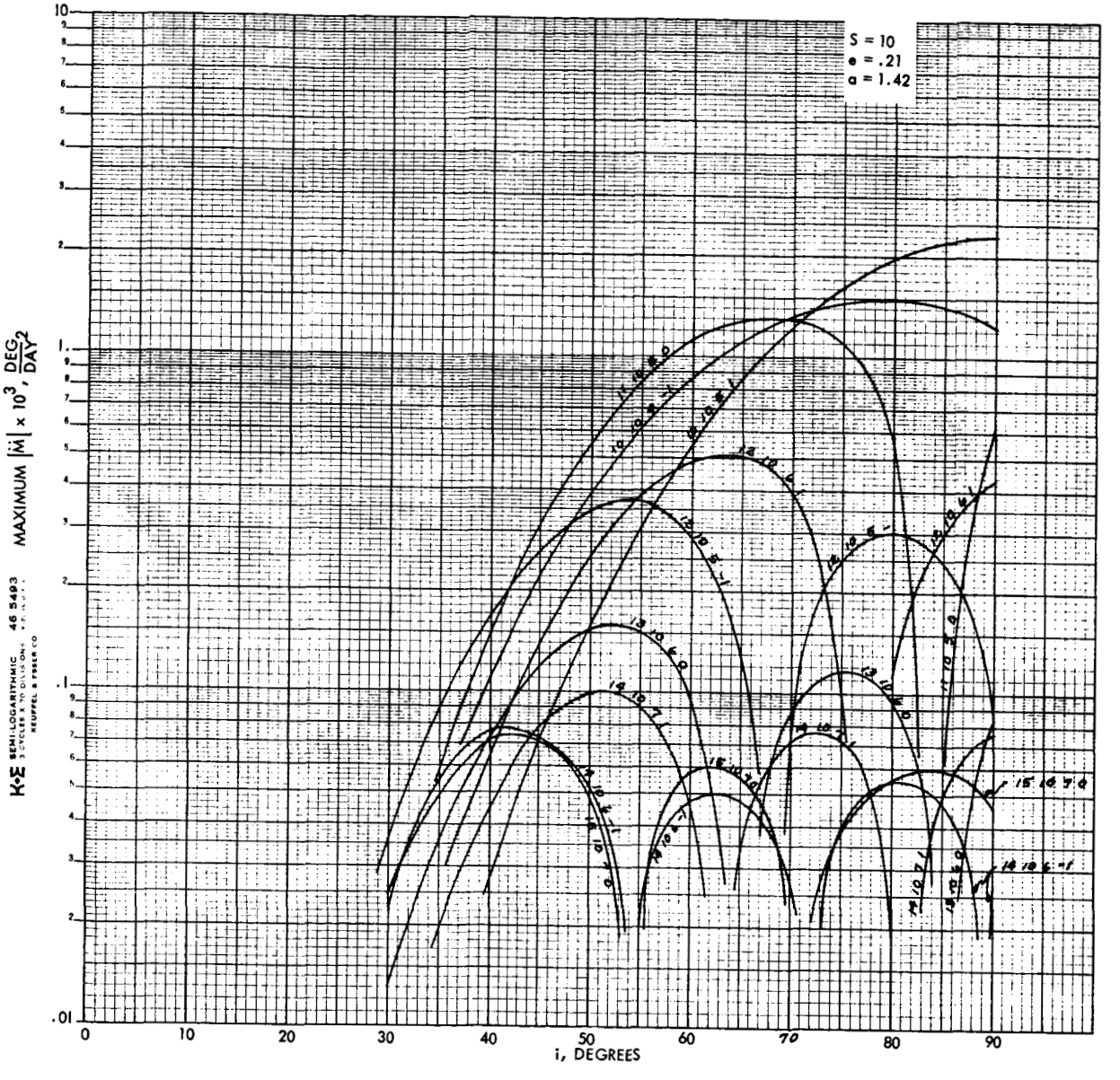
S = 10
e = .21
a = 1.42
MAXIMUM |M̈| x 10³, DEG/DAY²
i, DEGREES
10
9
8
7
6
5
4
3
2
1
.9
.8
.7
.6
.5
.4
.3
.2
.1
.01
0
10
20
30
40
50
60
70
80
90

Figure 3-16

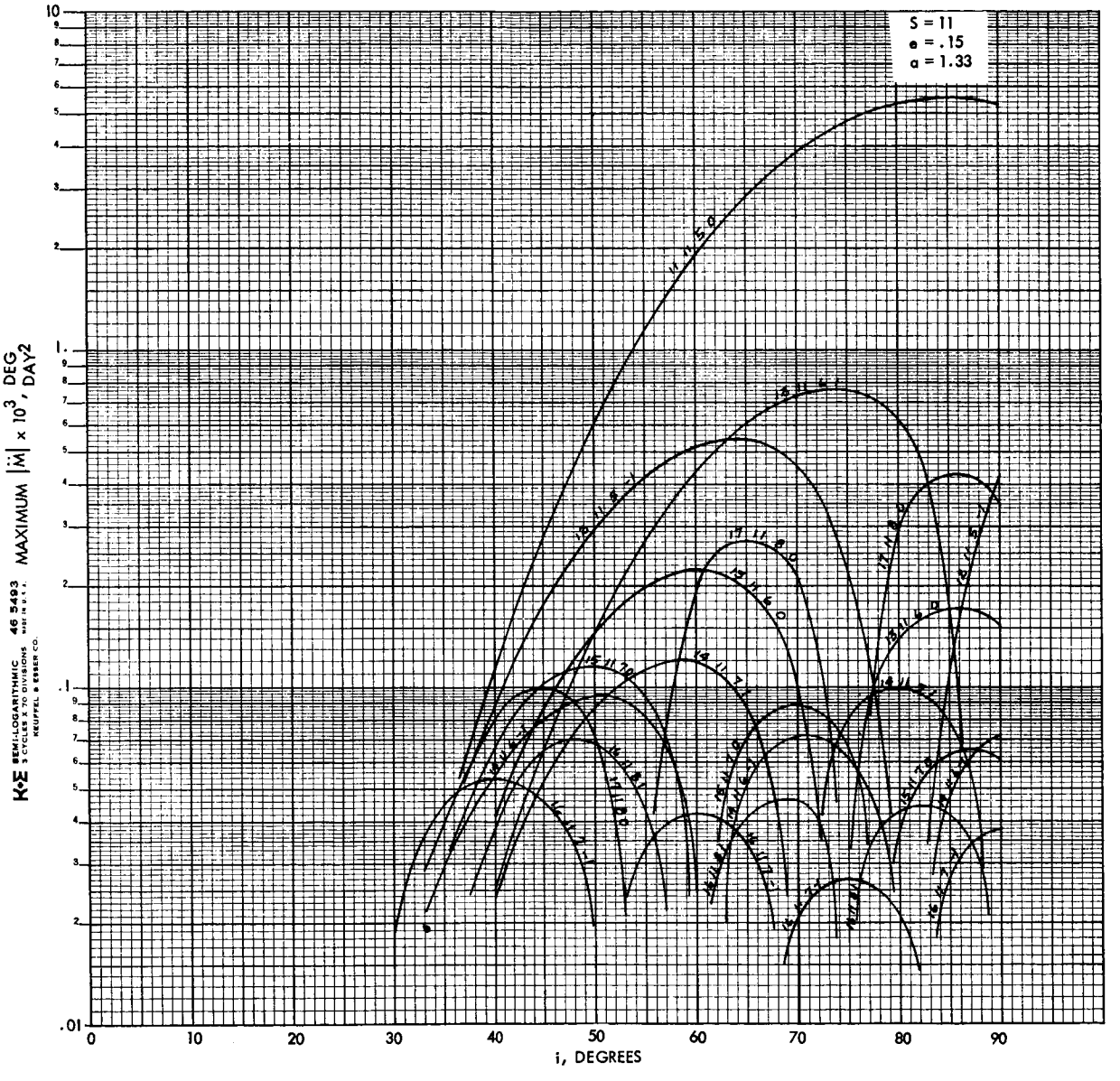
S = 11
e = .15
a = 1.33
MAXIMUM |M̈| x 10^3, DEG/DAY2
i, DEGREES
10
1.
.1
.01
0
10
20
30
40
50
60
70
80
90
K+E SEMI-LOGARITHMIC 46 5493
3 CYCLES X 70 DIVISIONS
KEUFFEL & ESSER CO.

Figure 3-17

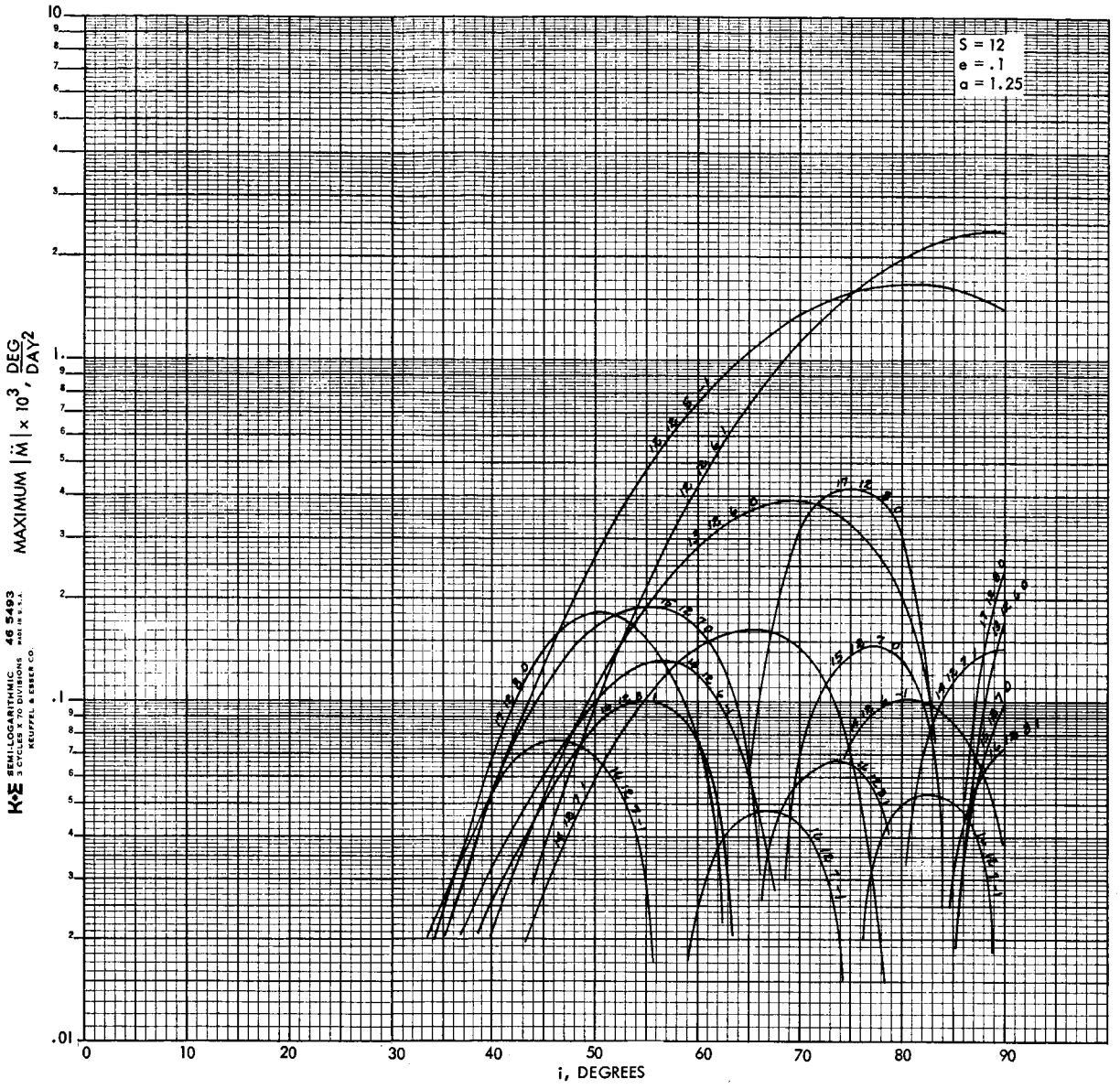
S = 12
e = .1
a = 1.25
MAXIMUM |M̈| x 10³, DEG/DAY²
i, DEGREES
10
9
8
7
6
5
4
3
2
1
.1
.01
0
10
20
30
40
50
60
70
80
90
K&E SEMI-LOGARITHMIC 46 5493
3 CYCLES X 70 DIVISIONS
KEUFFEL & ESSER CO.

Figure 3-18

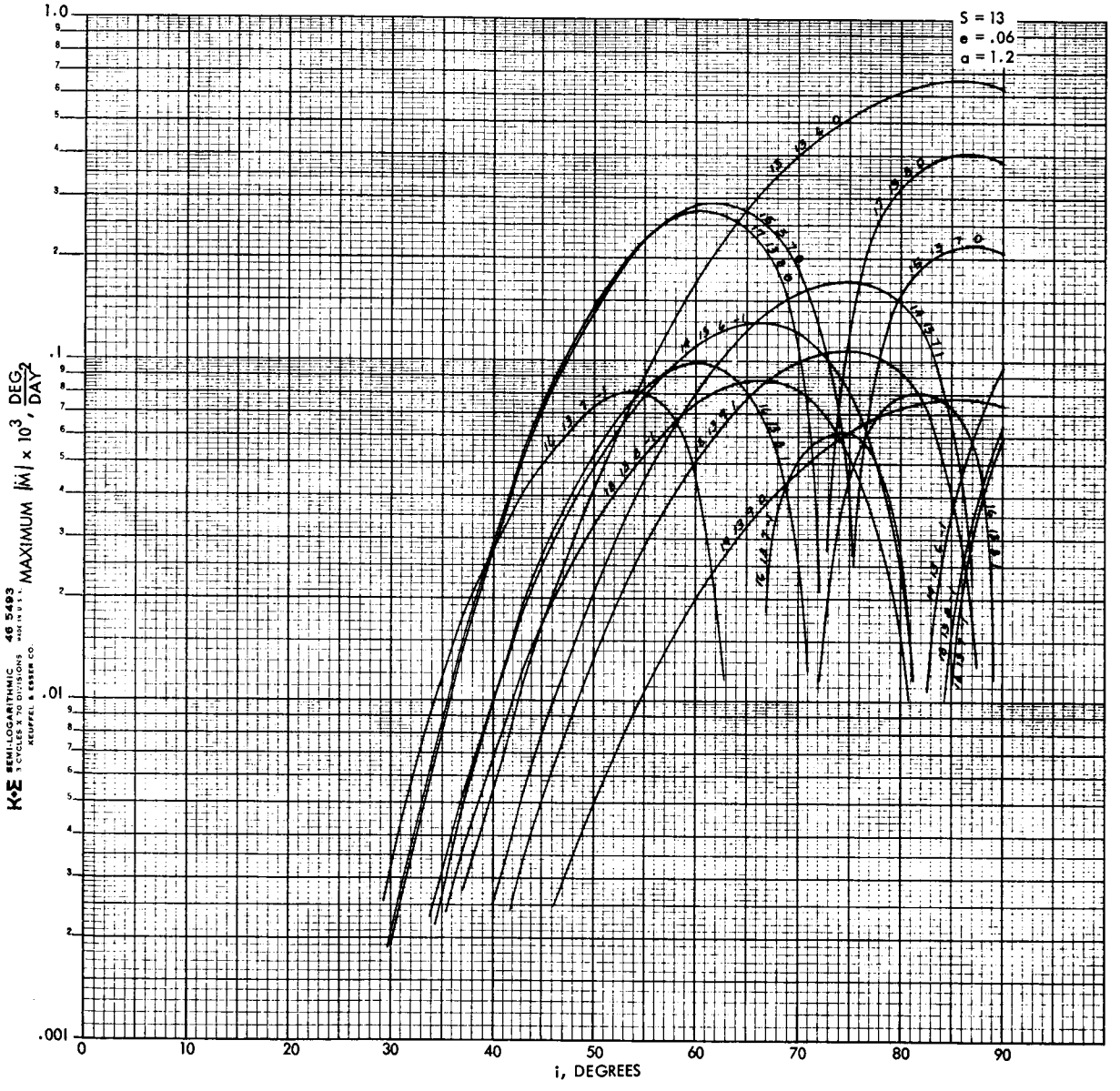
S = 13
e = .06
a = 1.2
MAXIMUM |M| x 10^3, DEG^2/DAY^2
i, DEGREES
1.0
.1
.01
.001
0
10
20
30
40
50
60
70
80
90
K&E SEMI-LOGARITHMIC 46 5493
3 CYCLES X 70 DIVISIONS
KEUFFEL & ESSER CO.

Figure 3-19

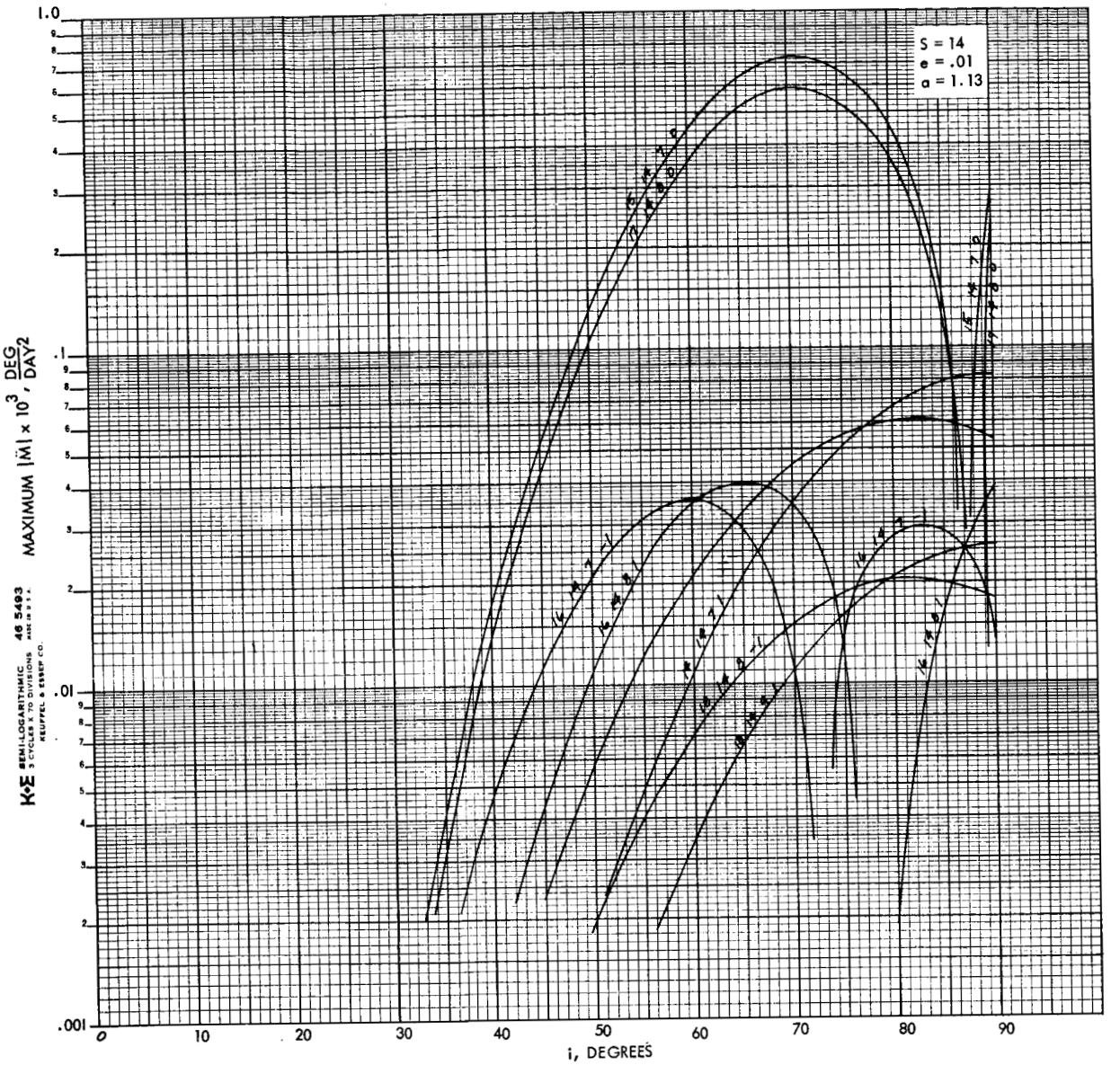
S = 14
e = .01
a = 1.13
MAXIMUM |M| x 10^3, DEG/DAY2
i, DEGREES
1.0
.1
.01
.001
0
10
20
30
40
50
60
70
80
90

Figure 3-20

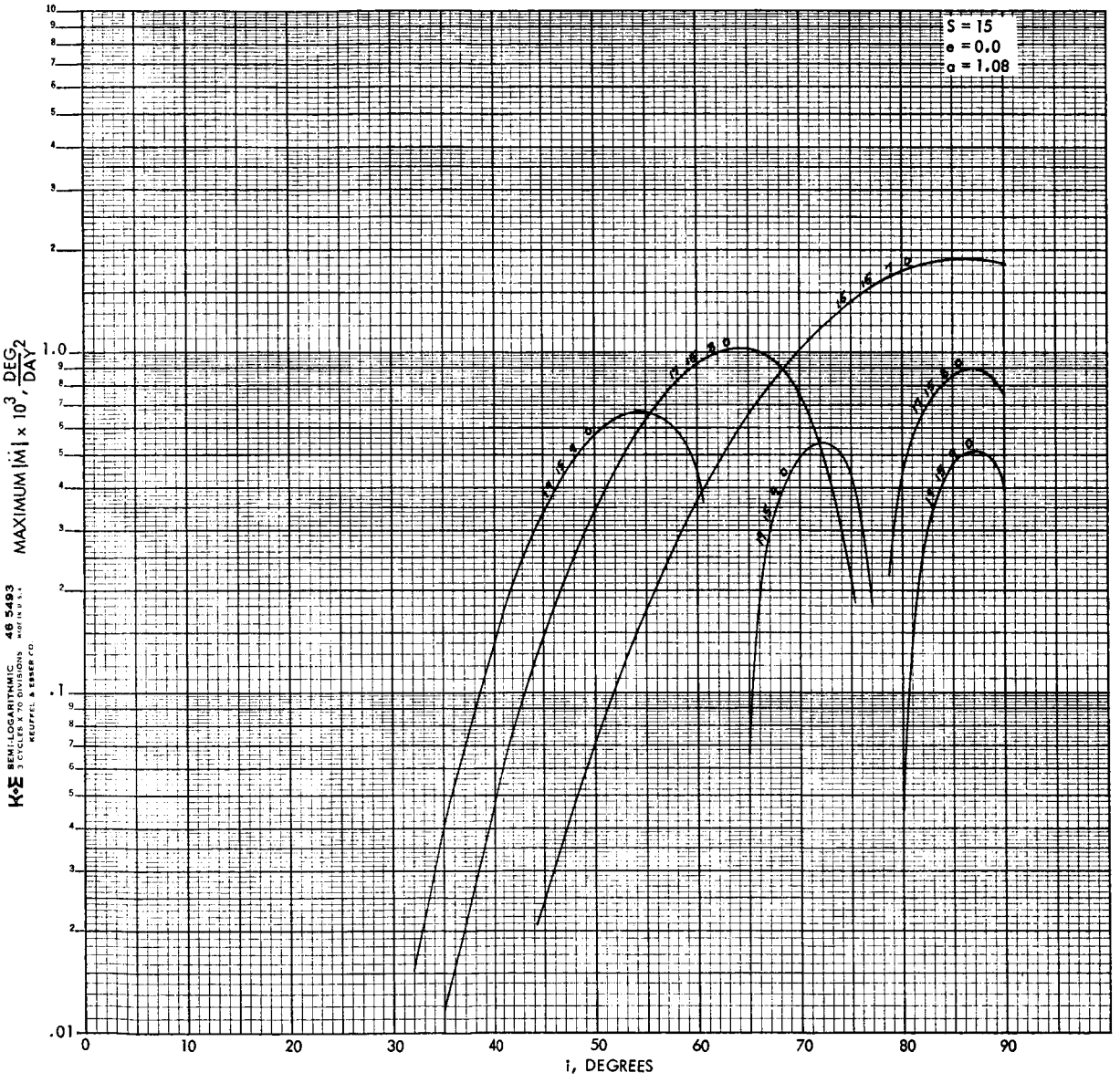
S = 15
e = 0.0
a = 1.08
MAXIMUM |M̈| x 10^3, DEG/DAY^2
i, DEGREES
0
10
20
30
40
50
60
70
80
90
1.0
.1
.01

Figure 3-21

4. ERROR ANALYSIS

The figure of merit for the comparison of resonant and nonresonant orbits in this study was the covariance matrix of the solution vector of geopotential constants. The advantage of the covariance matrix as a figure of merit is that it enables one to ascertain the effect of a large number of variable factors on the quality of a proposed orbit determination. In this study, the effects of period error, data rate, data span, and observation of multiple satellites on the covariance matrices of the resonant cases were studied.

The matrix equation expressing the orbit determination problem is given by

$$\delta R = A\delta X_A + B\delta Z_A + N \tag{4.1}$$

where δR is a column matrix of actual observations minus the reference observations. A is an n x p matrix, the elements of which are the partial derivatives of the observations (range, azimuth, elevation, etc.) with respect to the reference state vector at some epoch. (This state vector includes only the geopotential constants for this study). B is an n x m matrix, the elements of which are the partial derivatives of the observations with respect to the systematic errors. Systematic errors include the uncertainty in radar station location, biases in the observational data, and so forth. δX_A is a column matrix (p x 1) of deviations between the actual state vector at epoch and the reference state vector at epoch ($\delta X_A = X_A - X_R$). δZ_A is a column matrix (m x 1) of systematic errors and N is a matrix (n x 1) of the assumed Gaussian random noise with zero mean and known variance.

For this study, assume that $\delta Z_A = 0$. Then Equation 4.1 reduces to

$$\delta R = A\delta X_A + N \tag{4.2}$$

If W is a diagonal matrix whose elements are the reciprocals of the variances of the radar observations, then the weighted-least-squares estimate of the deviation from the reference (without a priori information) is

$$\delta X_E = (A^T W_A)^{-1} A^T W \delta R. \tag{4.3}$$

Substitution for δR from Equation 4.2 yields

$$\delta X_E - \delta X_A = (A^T W_A)^{-1} A^T W N. \tag{4.4}$$

The covariance matrix of the error in the estimated state vector due to tracking is

$$\Lambda_T = E(\delta X_E - \delta X_A)(\delta X_E - \delta X_A)^T. \tag{4.5}$$

Substituting Equation 4.1 into Equation 4.5 and making the assumption that $E(NN^T) = W^{-1}$, yields

$$\Lambda_T = (A^T W A)^{-1}. \tag{4.6}$$

The tracking normal matrix is then the inverse of the tracking covariance matrix, such that

$$S_T = (\Lambda_T)^{-1} = A^T W A. \tag{4.7}$$

The square roots of the diagonal elements of the covariance matrix are the standard deviations of the p components of the state vector.

In this study, the weighting matrix W was taken as the identity matrix. Thus the diagonal elements of the covariance matrix are equal to σ^2 (unknown)/ σ^2 (observation). The square root of this quantity was taken as the figure of merit.

If the covariance matrix is made to have unity diagonal terms, then the off-diagonal terms are correlation coefficients. Consideration of these quantities yields important insight into the conditioning of an orbit determination problem. The conditioning of the resonant satellite geodesy problem is explored in the results (Section 5).

This study is aimed at an evaluation of the relative usefulness of resonant and nonresonant orbits for geodesy. Therefore, many simplifying assumptions were possible.

First, the solution vector contained only the geopotential constants as unknowns. This restriction causes very optimistic results for nonresonant orbits and pessimistic results for resonant orbits, particularly those with orbital frequency above 12 revs/day. The reason for this is straightforward.

Effects of tesseral harmonics on a near-Earth nonresonant orbit are very small, ranging from at most a few hundreds of meters for the largest effect of the low degree terms such as (2, 2) to the order of a few tens of meters or less for very high degree terms. These effects, particularly for high degree terms, are comparable to such error sources as data biases, station location uncertainties, radiation pressure effects, and so forth. In the real world, we would expect these factors to seriously affect the determination of geopotential constants from nonresonant orbits. In contrast, the effects of resonant tesseral harmonics on resonant orbits are enormous compared to such error sources. Thus, neglect of these sources should be relatively much less important for resonant orbits.

Another factor leading to underestimation of the usefulness of resonant orbits is the neglect of short period effects in their computation. For high altitude resonant orbits, such as those with orbital frequencies of four, five, or less revs/day, the short period terms are very small and do not contribute much information, but for low altitude resonant orbits, for example, those with orbital frequencies of 12 revs/day or more, the resonant orbits are almost identical in character to the nonresonant orbits. Thus, the long period resonance effects are like extra sources of information.

Another way of expressing this is that for the pertinent resonant terms, low altitude resonant orbits experience short period perturbations of the same order of magnitude as nonresonant low altitude orbits plus additional very large resonant effects. Neglect of the short period terms for low altitude resonant orbits then must result in a conservative estimate of the usefulness of resonant orbits compared to nonresonant orbits.

A final simplifying factor in this analysis was the choice of data type. In both cases, a geocentric observer measuring along track position was assumed. This observation type is similar to conventional angle measurements and, since the same data type was used for both resonant and nonresonant orbits, a comparison is meaningful.

As previously indicated for nonresonant orbits, the partial derivatives of the observations with respect to the geopotential constants were obtained from analytic solution to the equations of motion. These solutions were differentiated with respect to the constants. Reference 17 gives a detailed treatment of analytic partial derivatives for orbit determination. These have been used successfully by the author of Reference 17 for determination of geopotential constants from real data.

For resonant orbits, partial derivatives were obtained by numerical differencing of nominal and perturbed trajectories. It was found that for orbital frequencies of 1 and 10 revs/day, perturbations in the constants of 2% to 5% yielded partial derivatives that were the same to at least three significant figures. For these cases, a perturbation of 3% was used. For an orbital frequency of 13 revs/day, much larger perturbations were needed because of the smaller effect of resonance on this orbit, compared to the other cases. Perturbations of 25% and 35% produced partial derivatives that also were the same in the third significant digit. The smaller figure was used. Note that for a 10-unknown covariance matrix one nominal and ten perturbed trajectories must be computed. For 300 days of a satellite with orbital frequency of 10 revs/day, 33,000 revs must be computed. The high speed program developed and used for this study accomplished this total calculation in about 6 min. of IBM 7094 computer time. The time required by a Cowell-type trajectory program would be nearly 8 hours.

5. RESULTS

In this study, three resonant orbits were considered. These are orbits having orbital frequencies of 1 rev/day, 10 revs/day, and 13 revs/day.

The first case, the so-called 24-hour orbit, was chosen for a special reason. A resonant, eccentric 24-hour orbit resonates with all terms in the geopotential. It is a matter of some interest to see actually how many of the terms have a perceptible effect. Also, such a resonant orbit gives a unique opportunity to determine from a resonant orbit those constants with the order (m) subscript equal to one.

The second case, 10 revs/day, was chosen as typical of those resonant orbits that resonate strongly with high degree ($\ell \geq 10$) terms in the geopotential but can still have substantial eccentricity while maintaining a drag-free perigee. The case of 13 revs/day was chosen as typical of those orbits that are resonant with very high degree terms ($\ell \geq 13$), but because of the necessity for drag-free perigee passage can have only low or zero eccentricity. As seen in Section 3, the magnitude of the eccentricity is very important to the strength of the resonance phenomenon. It is the small permissible eccentricity that causes a reduction in the usefulness of resonant orbits with $s \geq 13$, where s is orbital frequency.

Let us consider the 24-hour case first. Figure 5-1 shows the figure-of-merit, $\sigma_{unk.}/\sigma_{obs.}$ for 24-hour and near-Earth nonresonant satellite cases, both chosen to maximize the effect of the constants sought.

The inclination of 20° for the 24-hour satellite case was selected from the appropriate graph for 24-hour satellites. The inclination of 30° for the nonresonant orbit was found by experimentation, that is, a variety of covariance matrices for the nonresonant orbit were computed and the one showing the smallest variances was selected.

The constants C_{22}, S_{22} were not included in the solution vector because these particular constants are known very accurately from observations of both resonant and nonresonant orbits. Also, there is a serious separation problem for (2, 2) and (4, 2) for nonresonant orbits.

$\sigma_{unk.}/\sigma_{obs.}$ FOR RESONANT AND NONRESONANT ORBITS - 1

DATA SPAN 300 DAYS, 100 OBSERVATIONS

		NONRES	RESONANT
C_{31}	$\left(10^{-6}\right)$	.2E-1	.5E-1
S_{31}		.2E-1	.4E-1
C_{32}	$\left(10^{-7}\right)$	.1E-1	.2E-1
S_{32}		.2E-1	.3E-1
C_{33}	$\left(10^{-7}\right)$	.7E-2	.2E-1
S_{33}		.7E-2	.3E-1
C_{41}	$\left(10^{-7}\right)$	.1E-2	.1E0
S_{41}		.1E-2	.8E-1
C_{42}	$\left(10^{-7}\right)$	.2E-2	.6E-2
S_{42}		.2E-2	.1E-1

NONRESONANT: 500 MILE CIRCULAR, $i = 30°$

RESONANT: $a = 6.61231$ (24 HOUR ORBIT)
$e = 0.8$
$i = 20°$

Figure 5-1.

Figure 5-1 seems to suggest an unexpected result, viz., that for determination of low degree and order tersseral harmonics, a 24-hour orbit offers no advantage over a nonresonant orbit. However, there are factors which make this a pessimistic interpretation of the results.

As mentioned elsewhere in this report, the nonresonant effects of tesseral harmonics are very small and hard to observe. They are readily obscured by systematic errors. This study does not include consideration of these very important errors. Thus the results for the nonresonant orbit are probably quite optimistic. Only by observation of many nonresonant satellites at different inclinations over very long arcs has it been possible to determine these tesseral harmonic coefficients.

A glance at the column of results for the resonant-24-hour orbit in Figure 5-1 shows that the figure of merit $\sigma_{unk.}/\sigma_{obs.}$ does not decrease for the smaller constants at the end of the list. (The figures in parenthesis are the orders of magnitude of the constants.) This is not too surprising a result, since for 24-hour orbits the effect of a tesseral harmonic falls off very rapidly with increasing degree. The acceleration $\ddot{M}$ that produces the along track perturbation varies inversely with $a^{\ell+3}$. The semimajor axis, a, is 6.6 earth radii for the 24-hour orbit. Except for a few low degree terms in the geopotential, the 24-hour orbit cannot be very useful for geodesy because of this rapid drop off.

Let us now turn to a case of more immediate interest, the 2.4 hour orbit. This orbit is strongly resonant with terms of order (m) 10. Figure 5.2 shows the result.

The columns comparing the figure-of-merit for the resonant and nonresonant orbits are in striking contrast with Figure 5-1. Note that the figure-of-merit is two or three orders of magnitude smaller for the resonant cases. Since the figure of merit is proportional to the standard deviation of the unknown, the resonant solution is far superior to the nonresonant solution, especially so since this analysis has treated nonresonant orbits optimistically.

This result, in such contrast to the result for the 24-hour case, has a simple explanation. A glance at the graphs in Section 3 showing the accelerations of mean anomaly will show that the along track perturba-

$\sigma_{unk.}/\sigma_{obs.}$ FOR RESONANT AND NON-RESONANT ORBITS - II

DATA SPAN 300 DAYS, 60 OBSERVATIONS

		NON-RES	RES	RES, $\Delta V = 10$ FT/SEC	RES, $\Delta V = 30$ FT/SEC
$C_{10,10}$	$\left(10^{-16}\right)$	.4E-9	.2E-11	.2E-11	.3E-11
$S_{10,10}$		.5E-9	.5E-11	.2E-11	.6E-11
$C_{11,10}$	$\left(10^{-17}\right)$	.1E-9	.6E-12	.9E-12	.1E-11
$S_{11,10}$		.9E-10	.4E-13	.5E-12	.5E-12
$C_{12,10}$	$\left(10^{-17}\right)$	.3E-10	.7E-13	.8E-13	.1E-12
$S_{12,10}$		.2E-10	.2E-12	.9E-13	.3E-12
$C_{13,10}$	$\left(10^{-18}\right)$	.7E-11	.5E-13	.1E-12	.1E-12
$S_{13,10}$		.6E-11	.6E-13	.6E-13	.6E-13
$C_{14,10}$	$\left(10^{-19}\right)$	.3E-11	.9E-14	.7E-14	.1E-13
$S_{14,10}$		.3E-11	.2E-14	.9E-14	.2E-13

NON-RESONANT: 500 MILE CIRCULAR ORBIT, $i = 55°$

RESONANT: $a = 1.4197$ ($P = 2.4$ HRS)
$e = 0.21$
$i = 55°$

Figure 5-2.

tions due to the resonant tresseral harmonics on 2.4- and 24-hour orbits are comparable in magnitude, in spite of far smaller magnitudes of the coefficients. However, for nonresonant orbits, because of the very short period of even the longest period effect (period = 1/10 day), the perturbations on the nonresonant orbit have decreased with increasing degree (ℓ), decreasing the utility of the nonresonant orbit for geodesy.

For both the low degree (24-hour resonance) and high degree (2.4-hour resonance) cases, both data rate and data span were varied. The effect of data rate was just about that predictable on theoretical grounds, that is, doubling data causes halving of variances. For the nonresonant orbits, changing data quantity by increasing observation arc rather than reducing data interval had a similar effect. But for resonant orbits, the variances are more sensitive to data span. This, too, has a simple explanation. The resonance phenomenon is very long period, taking many months to develop into really large effects. By contrast, the nonresonant perturbations are essentially just reptitions of periodic phenomena. For the resonant case, information of a new character emerges as the various tesseral harmonic effects interact and distort each other. For the resonant 2.4-hour orbit, the figure-of-merit $\sigma_{unk}/\sigma_{obs}$ dropped by a full order of magnitude upon maintaining constant data rate but increasing data span from 150 to 300 days. Further increasing the data span to 450 days also had a favorable result, although not as large. To ascertain the data span necessary to determine the constants to some required accuracy from real data will require a careful error analysis that simulates the real world as accurately as possible. However, it is likely that observations over at least three to six months are required to allow the resonance phenomena to build up to large amounts.

The final case studied was the case of s = 13 revs/day. This case differs significantly from the s = 10 case because of the small permissible eccentricity (e = 0.06). This has the effect of reducing the perturbations (as can be seen from the graphs in section 2) and makes the orbit less useful for geodesy than the case of 10 revs/day. Comparing Figures 5-2 and 5-3, note that the figure-of-merit in the s = 10 case is about five orders of magnitude larger than the constant, and about 10 to 12 orders of magnitude larger for s = 13. Thus the s = 13 case will be much less

$\sigma_{unk.}/\sigma_{obs.}$ FOR S = 13 REVS./DAY

	DATA SPAN = 300 DAYS	DATA SPAN = 600 DAYS
$C_{13,13}$ $\left(10^{-20}\right)$	.2E-9	.9E-10
$S_{13,13}$	.2E-11	.4E-12
$C_{14,13}$ $\left(10^{-21}\right)$	.2E-08	.9E-9
$S_{14,13}$	.1E-08	.5E-9

a = 1.19377

e = .06

i = 85°

1 DATA PT. EACH 5 DAYS.

Figure 5-3.

useful. A decrease in usefulness is to be anticipated from the decreasing effect of resonance with increasing orbital frequency and subsequent lowering of eccentricity, but such a drastic difference was not expected and definitely calls for further study. Regardless, the s = 13 case must be more useful than a nonresonant orbit for the same constants. Our model for the resonant orbit ignores short period effects. Since the s = 13 resonant orbit has such small semimajor axis, it is practically identical with a geodetically useful nonresonant orbit. Thus, the resonance effects are really additional effects and will cause the resonant orbit to be more useful. It was for this reason that a nonresonant orbit was not compared for the s = 13 case.

The comparison of the s = 10 and s = 13 cases indicates that for constants of order 8, 9, 10, 11, and probably 12, eccentric resonant orbits will be very useful for determination of constants, yielding possibly one-fourth to one-third of the constants in the range (8, 8) to (15, 15). But for constants of orders 13, 14, 15, because of decreasing permissible eccentricity, the effects of only a smaller number of constants will be importantly enhanced. However, as seen, the cases of high degree, especially 13, 14, 15, so nearly resemble nonresonant orbits of geodetic usefulness that these orbits will still be more useful for geodesy than nonresonant orbits.

Of great interest are two remaining concerns of this study, viz, the effect of an injection velocity error, and the effect of combining observations of two satellites.

Figure 5-2 shows the effect of injection velocity errors of 10 ft/sec and 30 ft/sec upon the figure-of-merit of the case with s = 10 rev/day. The entire error was assumed to affect the period. Note that an error of 10 ft/sec has almost no effect on the results, and an error of 30 ft/sec has an effect of only about a factor of 2 in most cases. These large velocity errors are certainly within the range of many injection guidance systems and offer the possibility simple, of low cost satellites.

In the determination of geopotential constants, the question of separability of the constants from each other must arise, for this has been a great problem in the past for reduction of real data.

For nonresonant orbits, the problem arises because the dominant effects of two harmonics with the same order (m) subscript and degree subscripts (ℓ) differing by two oscillate with the same frequency. The other effects of the terms in question are very small and practically unobservable. Hence, separation is obtainable only by simultaneous processing of data from satellites at many inclinations.

For resonant orbits, the ill-conditioning problem should be less severe, because the perturbations are not simple linear additions to an intermediary orbit. The effects of terms with the same order (m) subscript are not exactly in phase with each other. This has been demonstrated by studying the correlation matrices associated with the covariance matrices of this study. The correlations are not 1.0, although they are occasionally as high as 0.999. This seems very high, but figures as high as this are often encountered in orbit determination problems from which useful information is obtained. What remains to be seen is the separability of the constants in the presence of systematic errors.

Because ill conditioning may be a problem if resonant orbits are to be of the utmost usefulness, it is important to study means of overcoming it. The basic means is to simultaneously consider data from two or more satellites with different orbital elements. The effects of the constants will bear different relationships to each other for the different orbits and hence, if considered simultaneously, will uncouple. The problem of ill conditioning was studied extensively for the case of s = 10 rev/day.

The three orbital elements whose variation is meaningful for the eccentric resonant orbit are a, e, and i. Only very small changes in semimajor axis are permissible to avoid completely destroying the resonance phenomenon. A case was studied in which the semimajor axis was varied by an amount corresponding to a perigee velocity change of 30 ft/sec. This amount is known not to seriously degrade the accuracy of the determination. Combining these cases, each of 300 days duration with one data point per five days resulted in only the result attributable to a doubling of the amount of data. The amount the semimajor axis could be varied was simply not great enough. Far different results were obtained with variation of e and i.

Figure 5-4 shows the effect of simultaneous reduction of data from two satellites with s = 10 revs/day at (1) inclinations of 55° and 70° and (2) eccentricities of 0.21 and 0.18. The combined estimates were obtained by addition of the appropriate normal matrices to form the normal matrix of the combined problem. This is equivalent to the assumption that the cases are uncorrelated. The nominal results for the single 2.4-hour orbit are repeated here for comparison. The effect is greater by orders of magnitude than would be expected from a mere doubling of the quantity of data, and the effect of eccentricity could be enhanced even more by a larger difference in eccentricity. If multiple satellites must be observed, there are real advantages to having them in the same orbit plane with different eccentricities rather than the usual situation of multiple orbit planes. Of course variations in eccentricity are limited to those resonant orbit cases having substantial eccentricity, viz., $s \leq 12$ revs/day.

The question of data types must also be considered. The resonance phenomenon manifests itself primarily as a large along-track effect. Thus, the choice of along-track position as data type for this study. This data type resembles, for example, Baker-Nunn Camera or Minitrack data, but absolute conclusions should not be drawn directly from the results.

Since this study was a relative one, it could be accomplished very economically by making many simplifying assumptions that had the effect of giving conservative estimates of the usefulness of eccentric resonance orbits for geodesy. One should not take the figures of merit for this study and convert them to standard deviations of the constants. This is especially true for the s = 10, 13 cases. For the case of low altitude orbits, a geocentric observer is, of course, much farther away from the satellite than an observer on the surface. For a given angular error, being farther away magnifies the amplitude of the implied error in position. It is also well known that the motion of the observer can be very important in orbit determination problems.

At first it might seem that angular data is the obvious choice because it directly measures the phenomenon of interest, that is, along track position. However, range and range-rate data are extremely accurate and of course, do not suffer the requirement of camera data that the

$\sigma_{unk.}/\sigma_{obs.}$ FOR OBSERVATION OF MULTIPLE SATELLITES

		(1) $\Delta i = 15°$	(2) $\Delta e = .03$	NOMINAL (1 ORBIT ONLY)
$C_{10,10}$	$\left(10^{-16}\right)$	.3E-13	.1E-12	.2E-11
$S_{10,10}$		.4E-14	.1E-12	.5E-11
$C_{11,10}$	$\left(10^{-17}\right)$	.1E-13	.1E-12	.6E-12
$S_{11,10}$		.2E-14	.5E-14	.4E-13
$C_{12,10}$	$\left(10^{-17}\right)$	.3E-14	.1E-13	.7E-13
$S_{12,10}$		.1E-14	.7E-14	.2E-12
$C_{13,10}$	$\left(10^{-18}\right)$	.2E-14	.1E-13	.5E-13
$S_{13,10}$		.3E-15	.7E-15	.6E-13
$S_{14,10}$	$\left(10^{-19}\right)$	.7E-15	.2E-14	.9E-14
$S_{14,10}$		.1E-15	.5E-15	.2E-14

S = 10 REVS/DAY

i = 55°, 80°

e = 0.21, 0.18

Figure 5-4.

observer be in darkness and the satellite in sunlight. Also, electronic data are much more abundant. It is not really possible to generalize about the optimum data type without a detailed study of the orbits in question, tracking networks, required accuracy of constants, and many other factors that affect data reduction problems.

In conclusion, this study has demonstrated that resonant orbits will be very useful for determination of many, but not all, of the constants in the range (8, 8) to (15, 15). To determine all the constants in this range will require a combined program of observation of both resonant and nonresonant orbits. Because the resonance effects are so large and of such an utterly different character than the effects of tesseral harmonics on nonresonant orbits, the constants obtained from resonant orbits will be extremely important. A large number of constants obtained very accurately from resonant orbits will result in a great reduction in the difficulty of the overall problem.

6. RECOMMENDATIONS FOR FURTHER STUDY

Having established that eccentric resonant orbits will be very useful for determination of geopotential constants in the range (8, 8) to (15, 15), the next logical step is a detailed error analysis that simulates the real world as closely as possible. This analysis should answer the following questions:

1. What are the significant error sources and their a priori covariances?

2. What are the effects of both solved-for and unsolved-for systematic errors on the quality of constants obtained from observation of satellites on resonant orbits?

3. What tracking network, data type, and observation schedule is optimum for a resonant satellite geodesy program?

4. How many satellites at different inclinations or eccentricities, if any, are needed to reduce the effect of ill conditioning to an acceptable level?

5. What are the precise injection guidance requirements for a resonant satellite system?

The answers to these questions will permit an accurate evaluation of the absolute accuracy to which constants can be obtained from satellites on eccentric resonant orbits.

APPENDIX A

Theory of Orbital Resonance

It is well known that repeating ground track (circular) satellite orbits exhibit a pendulum-type motion called libration due to tesseral harmonics in the potential of the earth. This paper shows that eccentric orbits, with periods commensurate or nearly commensurate with the rotation period of the earth are also subject to resonance effects, although their ground-track may not be repeating because of the rotation of the line of apsides.

Eccentric orbits are strongly perturbed by certain Fourier components of tesseral harmonics (called critical terms) which appear to rotate with respect to a planetary observer. Such critical terms produce not only libration (i.e., pendulum-like motion), but force the orbit to drift with the angular velocity with which the critical term rotates. However, when the amplitude of libration exceeds π/m, where m is the order of the tesseral harmonic in question, the "pendulum turns over"; instead of libration, circulation appears with an entirely different drift velocity, period, and amplitude.

In contrast with circular orbits, eccentric orbits are strongly perturbed by many critical terms. At small eccentricities or low inclinations a single term dominates, and a good analytic approximation is available. Near the "critical" inclination it is possible to combine the effects of all critical terms having the same frequency, permitting analytic solution. But the general case requires numerical integration for solution because the total effect of all the critical terms is not simply the sun of the individual effects. By numerically integrating only the long-period variations in the mean orbital elements, several hundred orbits can be calculated in a second on a high-speed automatic digital computer.

---

* This appendix was taken from "Resonance Effects on Eccentric Satellite Orbits," by G. S. Gedeon, B. C. Douglas, and M. T. Palmiter, Journal of the Astronautical Sciences, July-August 1967.

INTRODUCTION

Synchronous satellites on circular orbits are extensively used for communication and navigation purposes. This fact justifies the great attention that was given in the literature to orbital resonance which affects these satellites (see References 1-16). Subsynchronous satellites on eccentric orbits have found less application, though the Molniya series has eccentric orbits with periods very close to 12 hours. The existence of resonance for eccentric orbits is, of course, an interesting problem, since subsynchronous satellites on eccentric orbits do not have repeating ground-tracks due to the rotation of the line of apsides, except at the critical inclination.

This paper addresses itself to the above problem by generalizing the treatment followed in Reference 13. It is found in the present paper that commensurate satellites on eccentric orbits resonate with a greater number of tesseral harmonics than those on circular orbits. By observing such satellites over long arcs in time, it is possible that many tesseral harmonics could be determined with high accuracy.

On strictly or very nearly commensurate orbits the resonance is deep; all elements change which in turn affects the perturbing function (which is expressed with the Kepler elements of the orbit) especially through the large change in the mean anomaly. This can be regarded as a "feedback", and the resultant motion is a pendulum type of libration or circulation. For orbits far from commensurability the resonance is shallow, the changes are small, and the feedback on the perturbing function can be neglected. The observable motion is an along-track oscillation with an impressed period of a few days.

This paper will treat the case of deep resonance only. The effects of shallow resonance on eccentric orbits has been treated by Gedeon and Dial (Reference 16).

DISCUSSION

1. EQUATIONS OF MOTION

Kaula's formulation of the potential field of a planet in terms of the Kepler elements of the satellites is (see Reference 17):

$$V = \frac{\mu}{r} + \sum_{\ell=2}^{\infty} \sum_{m=o}^{\ell} \sum_{p=o}^{\ell} \sum_{q=-\infty}^{\infty} V_{\ell mpq} = \frac{\mu}{r} + R, \tag{1}$$

where

$$V_{\ell mpq} = \frac{\mu}{a} \left(\frac{a_e}{a}\right)^{\ell} F_{\ell mp}(i)\, G_{\ell pq}(e)\, J_{\ell m} \begin{cases} \cos \psi & (\ell-m)\text{even} \\ \sin \psi & (\ell-m)\text{odd} \end{cases} \tag{2}$$

and

$$\psi = [(\ell - 2p)\,\omega + (\ell - 2p + q)\,M + m\,(\Omega - \theta - \lambda_{\ell m})]. \tag{3}$$

In the above equation a, e, i, Ω, ω, M are the osculating Kepler elements, $F_{\ell mp}(i)$ is the inclination function and $G_{\ell pq}(e)$ is the eccentricity function. Expressions for these functions (which can be incorporated into a digital computer program) are given in Ref 17. For ease of analytical investigation, however, these are also tabulated in Ref 17 for $0 \leq \ell \geq 4$ and $-2 \leq q \leq 2$. The function $G_{\ell pq}(e)$ is of the order $e^{|q|}$: therefore the summation for q need be over only a few values near zero for orbits of low or moderate eccentricity. The rest of the symbols appearing in Equations (1), (2), and (3) are the following:

μ = gravitational constant

a_e = mean equatorial radius

r = position radius

$\theta = \theta_o + \dot{\theta} t$ = right ascension of Greenwich

$J_{\ell m}, \lambda_{\ell m}$ = coefficient and longitude of the major axis of symmetry of the (ℓ, m) spherical harmonic

Let us define now a number s by the following equation:

$$s(\dot{\theta} - \dot{\Omega}) = \dot{M} + \dot{\omega}. \tag{4}$$

Then s is essentially the number of satellite revolutions per Earth rotation. If $s = s_o + \Delta s$ where s_o is an integer, then

$$\frac{1}{s_o}(\dot{M} + \dot{\omega}) - (\dot{\theta} - \dot{\Omega}) = \frac{\Delta s}{s_o}(\dot{\theta} - \dot{\Omega}) = \dot{\lambda}_N. \tag{5}$$

The quantity $\dot{\lambda}_N$ can be interpreted as the rate of change of the osculating value of the longitude of the node of the mean satellite. Note that for eccentric orbits the node of the true satellite is quite different from that of the mean satellite, and if $\Delta s = o$, the orbit is exactly commensurate.

With Equation (5), the time derivative of the argument of the disturbing function, $V_{\ell mpq}$ can be rewritten as

$$\dot{\psi} = \left(\ell - 2p + q - \frac{m}{s_o}\right)(\dot{M} + \dot{\omega}) + m\dot{\lambda}_N - q\dot{\omega}. \tag{6}$$

If

$$\ell - 2p + q = \frac{m}{s_o}, \tag{7}$$

the short period terms disappear, leaving only long period ones for commensurate and near commensurate orbits. The indices which satisfy Equation (7) define the critical $V_{\ell mpq}$ perturbing terms. For such terms:

$$\dot{\psi} = m\dot{\lambda}_N - q\dot{\omega}. \tag{8}$$

Note that for strictly commensurate orbits $\dot{\lambda}_{No} = 0$.

Because the rates $\dot{\Omega}$, $\dot{M}$ and $\dot{\omega}$ do not necessarily remain constant under the action of the tesseral harmonics, it is necessary to consider the acceleration

$$\ddot{\lambda}_N = \ddot{\Omega} + \frac{1}{s_o}(\ddot{M} + \ddot{\omega}) . \tag{9}$$

Designating the Keplerian elements by α_i where $i = 1,\ldots,6$, the second rate of change of an element can be written as

$$\frac{d^2\alpha_i}{dt^2} = \sum_{j=1}^{6} \frac{\partial \dot{\alpha}_i}{\partial \alpha_j}\frac{d\alpha_j}{dt} + \frac{\partial \dot{\alpha}_i}{\partial t} , \tag{10}$$

or in more detail as

$$\frac{d^2\alpha_i}{dt^2} = \frac{\partial \dot{\alpha}_i}{\partial \psi}\dot{\psi} + \sum_{a_j = a,e,i} \frac{\partial \dot{\alpha}_i}{\partial \alpha_j}\dot{\alpha}_j . \tag{11}$$

Now $\dot{\alpha}_i$ and hence $(\partial\dot{\alpha}_i/\partial\psi)$ are of order $J_{\ell m}$; and $\dot{\psi}$ for commensurate orbits and critical indices is very small. The order of the products in the summation is $O(J_m)^2$ with the notable exception of $(\partial\dot{M}/\partial a)\dot{a}$. This partial contains a zero order term

$$\frac{\partial \dot{M}}{\partial a} = \frac{\partial n}{\partial a} = -\frac{3}{2}\frac{n}{a} , \tag{12}$$

which is multiplied by $\dot{a}$ as given by Lagrange's Planetary Equation (see, e.g., Ref 17

$$\frac{da}{dt} = \frac{2}{na}\frac{\partial R}{\partial M} . \tag{13}$$

Thus, when the condition for resonance is met, the second derivative of the mean anomaly can be approximated closely by

$$\ddot{M} \cong -\frac{3}{a^2}\sum \frac{\partial V_{\ell mpq}}{\partial M} . \tag{14}$$

Since $\ddot{M}$ is the only second derivative which is of order $J_{\ell m}$, it will dominate Equation (9). Equation (14) is approximate only, because terms $O(J_{\ell m}\dot{\psi})$ and $O(J_{\ell m})^2$ have been neglected.

Noting that $\ddot{M} \cong s_o \ddot{\lambda}_N$ (Equation 4), Equation (14) can be put in the following form:

$$\ddot{\lambda}_N \cong -\frac{1}{s_o}\frac{3}{a^2}\frac{\mu}{a}\sum (\ell - 2p + q)\left(\frac{a_e}{a}\right)^{\ell} F_{\ell mp}(i)\, G_{\ell pq}(e)\, J_{\ell m} \begin{bmatrix} -\sin\psi \\ \cos\psi \end{bmatrix}^{(\ell-m)\text{odd}}_{(\ell-m)\text{even}} . \tag{15}$$

Noting that $\ell - 2p + q = m/s_o$ for the critical indices, $\mu = n^2 a^3$ and $n \cong 2\pi s_o$, Equation (15) can be written as

$$\ddot{\lambda}_N \cong \sum m\left(\frac{2\pi m}{P_{\ell mpq}}\right)^2 \begin{bmatrix} \sin\left[\psi + (1+\xi)\,\pi/2\right] \\ \sin\left[\psi + \xi\,\pi/2\right] \end{bmatrix}^{(\ell-m)\text{odd}}_{(\ell-m)\text{even}} , \tag{16}$$

where

$$P_{\ell mpq} = \frac{1}{m}\left[\frac{(a/a_e)^{\ell}}{3\left|F_{\ell mp}(i)G_{\ell pq}(e)\right|J_{\ell m}}\right]^{1/2} \text{days}, \tag{17}$$

and

$$\xi = \begin{Bmatrix} +1 \\ -1 \end{Bmatrix} \text{ if } F_{\ell mp}(i)\, G_{\ell pq}(e) \begin{Bmatrix} > \\ < \end{Bmatrix} 0 . \tag{18}$$

The summation is for the critical indices which define ψ for commensurate orbits as the integral of Equation (8)

$$\psi = m(\lambda_N - \lambda_{\ell m}) - q\omega. \tag{19}$$

Equation (16) for such indices becomes

$$\ddot{\lambda}_N \cong -\sum m\left(\frac{2\pi/m}{P_{\ell mpq}}\right)^2 \sin m(\lambda_N - \bar{\lambda}_{\ell m}). \tag{20}$$

where

$$\bar{\lambda}_{\ell m} = \lambda_{\ell m} + \frac{2\pi k}{m} - \begin{cases} (1+\xi)\frac{\pi}{2m} & (\ell-m)\text{even} \\ \xi\frac{\pi}{2m} & (\ell-m)\text{odd} \end{cases} + \frac{q}{m}\omega_o + \frac{q}{m}\dot{\omega}t \tag{21}$$

In Reference 13, q was zero because of the restriction to circular orbits. Thus, $\bar{\lambda}_{\ell m}$, (which was interpreted as the stable node), was stationary. For eccentric orbits with $q \neq 0$, $\bar{\lambda}_{\ell m}$ rotates with the $\frac{q}{m}\dot{\omega}$ uniform angular velocity.

2. SOLUTION FOR A SINGLE CRITICAL TERM

Equation (20) for a single critical term can be regarded as the differential equation of an m-fold pendulum with a forcefield rotating with $(\frac{q}{m}\dot{\omega})$ angular velocity in the equatorial plane. Transforming to a coordinate system rotating with this velocity eliminates the explicit appearance of the time. Thus, in the rotating frame, Equation (20) becomes autonomous. (This is a similar situation to that of the restricted three body problem where the Lagrangian is rheonomic in an inertial coordinate system, but scleronomic in the system rotating with the angular velocity of the two massive bodies.)

The transformation consists of the introduction of a new variable, x, by the following definition:

$$x \triangleq \lambda_N - \bar{\lambda}_{\ell m} \cdot \tag{22}$$

Since $\ddot{\omega}$ is negligibly small, $\ddot{\lambda}_N = \ddot{x}$ and Equation (20) for a single tesseral becomes

$$\ddot{x} + mu_o^2 \sin mx = 0 \ , \tag{23}$$

where

$$u_o = \frac{2\pi/m}{P_{\ell mpq}} \ . \tag{24}$$

Equation (23) admits a first integral

$$\dot{x}^2 = C + 2u_o^2 \cos mx \ , \tag{25}$$

with C evaluated from the initial conditions, i.e.,

$$C = \dot{\bar{\lambda}}_{No}{}^2 - 2u_o{}^2 \cos m\,(\lambda_{No} - \bar{\lambda}_{\ell m_o}) \ , \tag{26}$$

where

$$\dot{\bar{\lambda}}_{No} = \dot{\lambda}_{No} + \frac{q}{m}\dot{\omega}, \tag{27}$$

is the modified initial drift rate which accounts for the advancement of the perigee.

If

$$C < 2u_o^2$$

the longitude of the node of the mean satellite relative to the rotating frame will librate as a pendulum, because for an $x = \alpha$ defined by

$$\cos m\alpha = - \frac{C}{2u_o^2}, \tag{28}$$

$\dot{x}$ becomes zero in Equation (25). For this case the integral can be written in the form

$$\dot{x}^2 = 4u_o^2 \left(\sin^2 \frac{m}{2}\alpha - \sin^2 \frac{m}{2} x\right), \tag{29}$$

and the period can be obtained through the introduction of the auxiliary variable ϕ defined by

$$\sin\phi = \frac{\sin m x/2}{\sin m\alpha/2}. \tag{30}$$

Then Equation (29) can be integrated between fixed limits as:

$$P = \frac{2}{\pi} P_{\ell mpq} \int_o^{\pi/2} \frac{d\phi}{\left[1 - k^2 \sin^2\phi\right]^{1/2}} = \frac{2}{\pi} P_{\ell mpq} K(k), \tag{31}$$

where $P_{\ell mpq}$ represents the period of small amplitude libration (see Figures 1,2), and k is the modulus defined by

$$k = \sin m\frac{\alpha}{2} = \left[\frac{C + 2u_o^2}{4u_o^2}\right]^{1/2} . \tag{32}$$

The quantity K(k) is a complete elliptical integral of the first kind.

If

$$C > 2u_o^2 ,$$

$\dot{x}^2$ is always positive and the pendulum turns over, i.e., the longitude of the node of the mean satellite circulates in the rotating coordinate system. In this case, Equation (25) can be readily integrated as

$$P = \int_o^{2\pi/m} \frac{dx}{\left[C + 2u_o^2 \cos mx\right]^{1/2}} \tag{33}$$

The above equation can be also converted into the form

$$P = \frac{k'}{\pi} P_{\ell mpq} K(k') \tag{34}$$

where

$$K(k') = \int_o^{\pi/2} \frac{d\phi'}{\left[1 - k'^2 \sin^2 \phi'\right]^{1/2}} \tag{35}$$

is a complete elliptical integral of the first kind,

$$k' = \left[\frac{4u_o^2}{C + 2u_o^2}\right]^{1/2} = \frac{1}{k} , \tag{36}$$

and

$$\phi' = \frac{m}{2} x. \tag{37}$$

From the period, the mean relative drift rate is

$$u_r = \frac{2\pi/m}{P} \quad . \tag{38}$$

The absolute drift rate, u_{ab}, is given by

$$u_{ab} = u_r + \frac{q}{m}\dot{\omega} \quad . \tag{39}$$

To find the amplitude of the angular irregularity of the overturning pendulum, Equation (33) must be rewritten in a non-complete elliptic integral form:

$$t = \frac{k'}{nu_o}\int_0^{\phi'} \frac{d\phi'}{[1 - k'^2\sin^2\phi']^{1/2}} = \frac{k'}{2\pi} P_{\ell mpq} F(k', \phi'). \tag{40}$$

The inverse of the above equation is $\phi' = f(t)$. If $\phi'_r = \frac{m}{2} u_r t$ is subtracted, the result is the angular irregularity

$$\Delta\phi' = f(t) - \frac{m}{2} u_r t. \tag{41}$$

To obtain the amplitude of the angular irregularity of circulation, the first derivative of Equation (41) should be equated to zero.

$$\frac{d\Delta\phi'}{dt} = f(t) - \frac{m}{2} u_r = 0. \tag{42}$$

But

$$f'(t) = \frac{1}{dt/d\phi'} = \frac{mu_o}{k'}\left[1 - k'^2\sin^2\phi'\right]^{1/2} . \tag{43}$$

Thus the angular position for the maximum of the deviation is obtained from

$$\sin \phi'_m = \frac{1}{k'} \left[1 - \left(\frac{\pi/2}{K(k')} \right)^2 \right]^{1/2} \tag{44}$$

The corresponding amplitude is obtained by calculating t_m from Equation (40) and $\Delta\phi'_m$ from

$$\Delta\phi'_m = \phi'_m - \frac{m}{2} u_r t_m . \tag{45}$$

Small amplitude librations showing orbital inclinations versus periods in years are given in Figures 1 and 2.

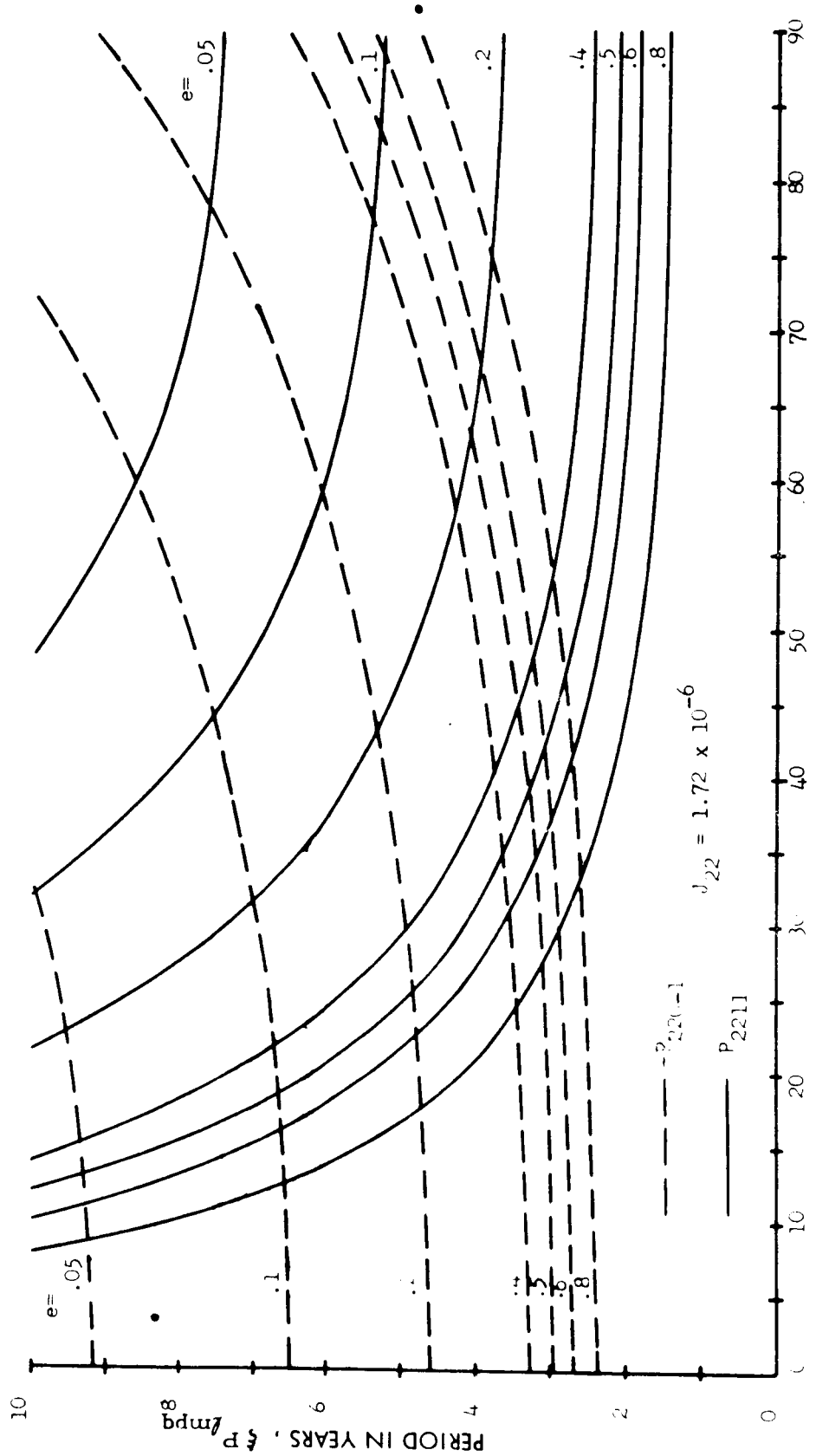

Figure 1. Small Amplitude Libration Periods of 12 Hour Orbits for V_{220-1} and V_{2211}

(41)

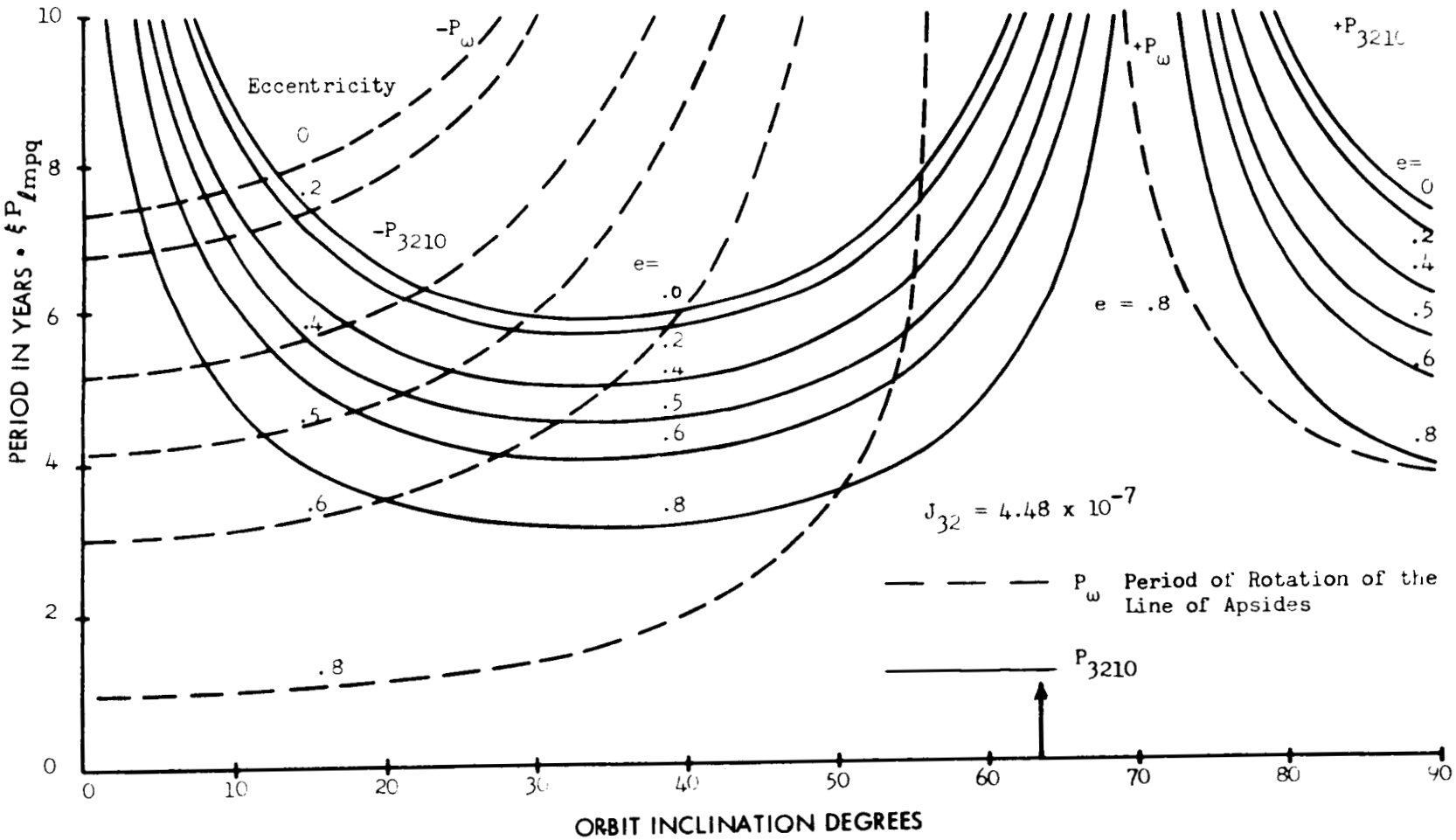

Figure 2. Small Amplitude Libration Periods of 12 hour Orbits for V_{3210} and the Period of Rotation of the Line of Apsides.

3. INTERPRETATION OF THE LIBRATION PHENOMENON

The phenomenon of libration is considerably more complicated than the forced vibration of a mass-spring system, where the approach to resonance manifests itself with an every-increasing amplitude.

In the case of libration there is a feedback between the orbit and the perturbing tesseral harmonics through Equation (9). The critical harmonic changes all the elements, but especially the mean anomaly. Thus, resonance affects the forcing function. The ensuing motion resembles that of a pendulum which oscillates or turns over on its axis. The amplitude is determined by the initial position and velocity, the period by the orbital parameters, the coefficient of the critical harmonic, and the amplitude.

An attempt will be made now to give a physical analogy of the librational phenomenon. First, it must be noted that the potential field is characterized by only two numbers $J_{\ell m}$ and $\lambda_{\ell m}$, but in the above treatment four indices (ℓ, m, p, q) were used to define resonance. This can be explained by the analogy to harmonic analysis. The disturbing function is expanded into a Fourier series in the mean anomaly. Equation (1) is the result of a Fourier series expansion of the standard form of the potential, after a coordinate transformation which introduced p.

For an analogy of libration, Figure 3 was conceived. It reproduces the gross characteristics of the phenomenon, although the time history of its motion is not the same. On Figure 3 the equatorial irregularity associated with a $J_{\ell m}$ is represented by a "hoop" with m "highs" and m "lows" upon which a frictionless roller is moving under the influence of a central spring. The $\xi = -1$ case, which produces positive central perturbing forces, can be simulated by placing the roller inside the path with the spring under compression. Then the stable equilibrium nodes will be at the highs.

For orbits with $q\dot{\omega} = 0$ (circular orbits, or critical inclination) the force field of the critical term appears to be stationary for an observer on the earth. For this case the hoop is also stationary.

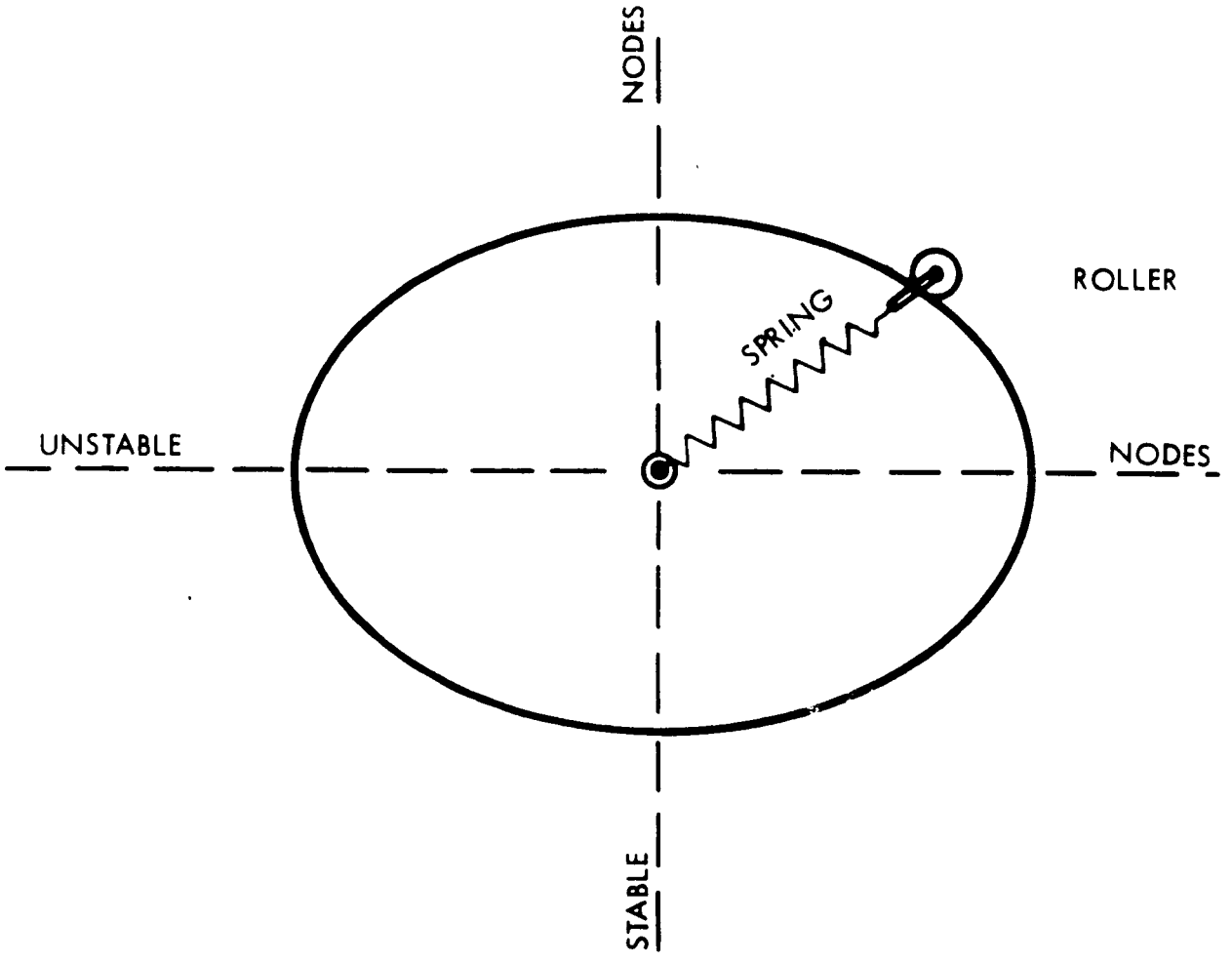

Figure 3. Simulation of the Gross Characteristics of Libration

If the roller is initially at a low, it is in equilibrium. But if it is displaced by a new initial position or by an initial velocity or a combination of both, it will start to oscillate around the stable node and its period will increase with the amplitude reaching infinity for $\alpha = \pi/m$.

If $q\dot{\omega} \neq 0$ then the force field of the critical term is time dependent. On Figure 3 the "hoop" must be turned on to rotate with a $(\frac{q}{m}\dot{\omega})$ rate to simulate the field of the critical term. Now if $\dot{\bar{\lambda}}_{No} = \dot{\lambda}_{No} + \frac{q}{m}\dot{\omega}$ is small and the roller was close to the stable equilibrium position the result is a libration with greater amplitude than the initial displacement. Note, however, that the roller will be carried along by the hoop. When the amplitude calculated by Equation (28) becomes greater than π/m the roller goes over the nearest high and begins to circulate. Since it circulates and is not carried along by the hoop its mean velocity will be the difference between the mean circulation velocity and the hoop velocity.

Physically, the satellite librates because the gravitational field rotates with the planet. Because the satellite period is commensurate with the Earth's rotation period, this feeds energy in and out of the satellite. Due to this energy change the semi-major axis of the orbit changes, which changes the period. A change in period affects the along-track position which in turn changes the longitude of the ascending node.

4. INFLUENCE OF THE INITIAL CONDITIONS

a) Initial Longitude, λ_{No}.

For critical tesserals with q = 0 the influence of initial longitude can be easily assessed since the angular distance between the initial longitude of the ascending node of the mean satellite, λ_{No} and the nearest stable node $\bar{\lambda}_{\ell m}$ is the amplitude. Where $q \neq 0$ the problem is more complicated because the differential equation of motion contains the time explicitly.

A numerical example was chosen to illuminate such a case: 12 hour, 30 degree inclined, e = 0.5 orbit, perturbing critical tesseral term V_{220-1}. Small amplitude libration period from Fig. A.1 is $P_{220-1} = 3.163$ years and the period of the perigee advancement from Fig. A.2 is $P_{\omega} = 6.007$ years. With these

$$u_o = 1.993 \text{ and } \dot{\omega} = 1.046 \text{ rad/year} \quad \dot{\bar{\lambda}}_{No} = -.523. \text{ rad/year}$$

Starting with $(\lambda_{No} - \bar{\lambda}_{\ell m_o}) = 0$ and continuing with incrementing the angular distances from the stable node, a point is found where $\cos 2\alpha = -1$. Up to this point the longitude of the ascending node of the mean satellite librates with increasing α amplitude and increasing period in an equatorial coordinate system rotating with -.523 rad/year angular velocity.

The point where $\cos 2\alpha = -1$ corresponds to $\lambda_{No} - \bar{\lambda}_{\ell m_o} = 74.7$ degrees. The amplitude is 90 degrees and the period is infinity. Beyond this point the pendulum λ_N circulates and the behavior of motion is markedly changed. At the unstable node, for example, the energy constant is C = 2.246, the modulus is k' = .967, and the complete elliptic integral of the first kind is K(k') = 2.784. Thus, the period becomes P = 2.71 years. If the λ_N circulates in 2.71 years its mean drift velocity is $u_r = 1.16$ rad/year.

The amplitude of the circulation irregularity in case the "pendulum turns over" is the maximum deviation from the mean. This can be calculated as $\phi'_m = 58.6$ degrees, $F(k', \phi') = 1.241$, $t_m = .604$, $\Delta\phi'_m = 18.5$ degrees.

Figure 4 shows the amplitudes, periods and drift rates for different initial values of the node. Figure 5 shows the time history of libration due to V_{220-1} obtained by the RESORB Program, which numerically integrates long-period contributions to Lagrange's Planetary Equations. The stable node is $\bar{\lambda}_{22_o} = 167$, since $\xi = -1$ and $\omega_o = 0$.

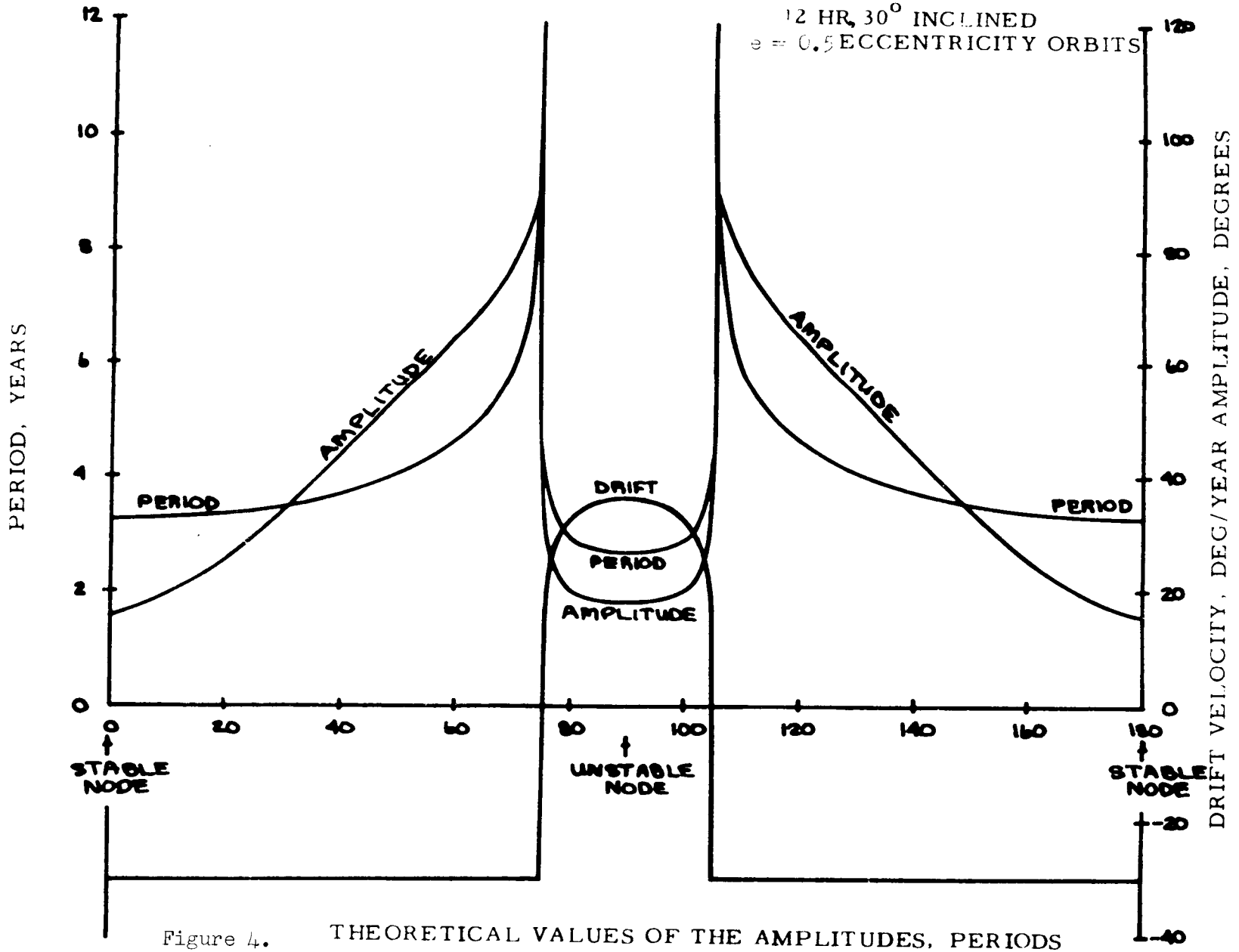

Figure 4. THEORETICAL VALUES OF THE AMPLITUDES, PERIODS AND DRIFT VELOCITIES DUE TO V_{220-1}

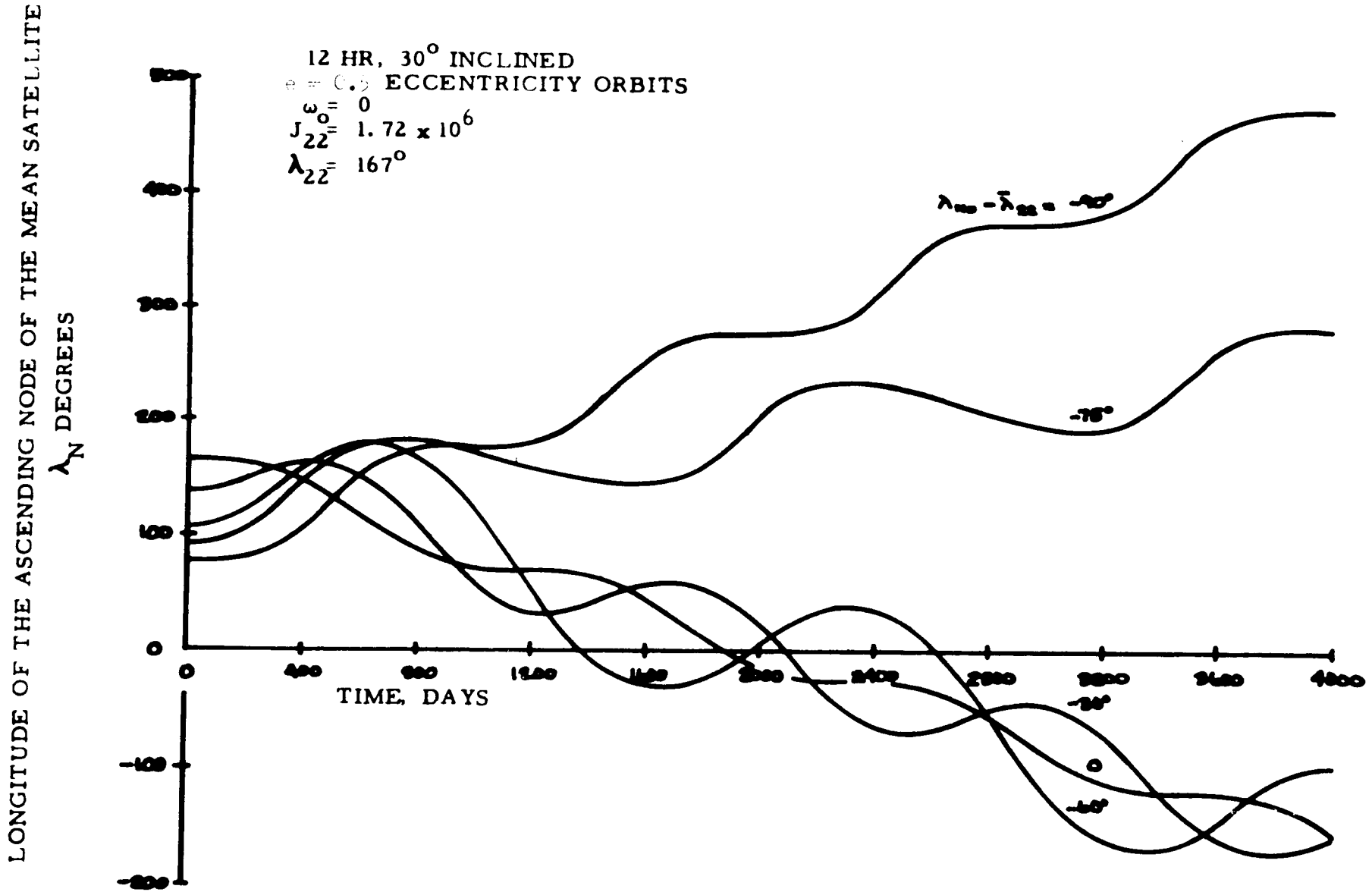

Figure 5. LIBRATIONS DUE TO V_{220-1}

It can be seen that with increasing $(\lambda_{No} - \bar{\lambda}_{\ell m_o})$ the amplitude and period increase and the drift rate remains constant and equal to the $-\frac{\dot{\omega}}{2}$ value. But at 75 degrees λ_N circulates, the drift rate changes drastically and the libration curve is skewed (it is not symmetrical). At 90 degrees the amplitude of circulation is the smallest because the pendulum rotates the fastest. Amplitudes, periods, drift rates obtained from these runs are in perfect agreement with Figure 4.

Runs made with λ_{No} at equal distance from the stable nodes revealed a perfect symmetry of the motion with respect to the stable node.

Figure 6 illustrates librations of a 12 hour, e = .5 eccentricity orbit at the critical inclination under the influences of V_{2211}. The stable node is at 77 degrees. As expected, there is no drift velocity because $\dot{\omega} = 0$ and the orbit is perfectly commensurate for all initial values of the node except that of 167 degrees which corresponds to the unstable node. At this point the slightest amount of targeting error (in the semi-major axis) makes the pendulum turn over, as can be seen on Figure 6. As soon as the initial longitude of the node has passed the unstable node, the libration in the normal manner appears, as shown by the λ_{No} = 197 degree curve.

Note that for the circulation the mean drift velocity is not the small drift velocity caused by mistargeting, but the much larger value of the mean circulation minus the initial drift rate.

For eccentric orbits, charts similar to Figure 4 can be made for V_{320-2} and V_{3222} with $\mp$ 60 °/year apparent force field rotation. It will be seen later that λ_N circulates for almost all λ_{No} values, producing a very small absolute drift rate. This, coupled with the fact that P_{320-2} and $P_{3222} >> P_{3210}$ diminishes considerably the importance of these higher terms for all values of λ_{No} except in the vicinity of the stable node. Finally, for critical tesserals with $|q| > 2$ computer runs were made with RESORB, which show hardly any trace of resonance, because of the fast circulation rate and the small eccentricity function.

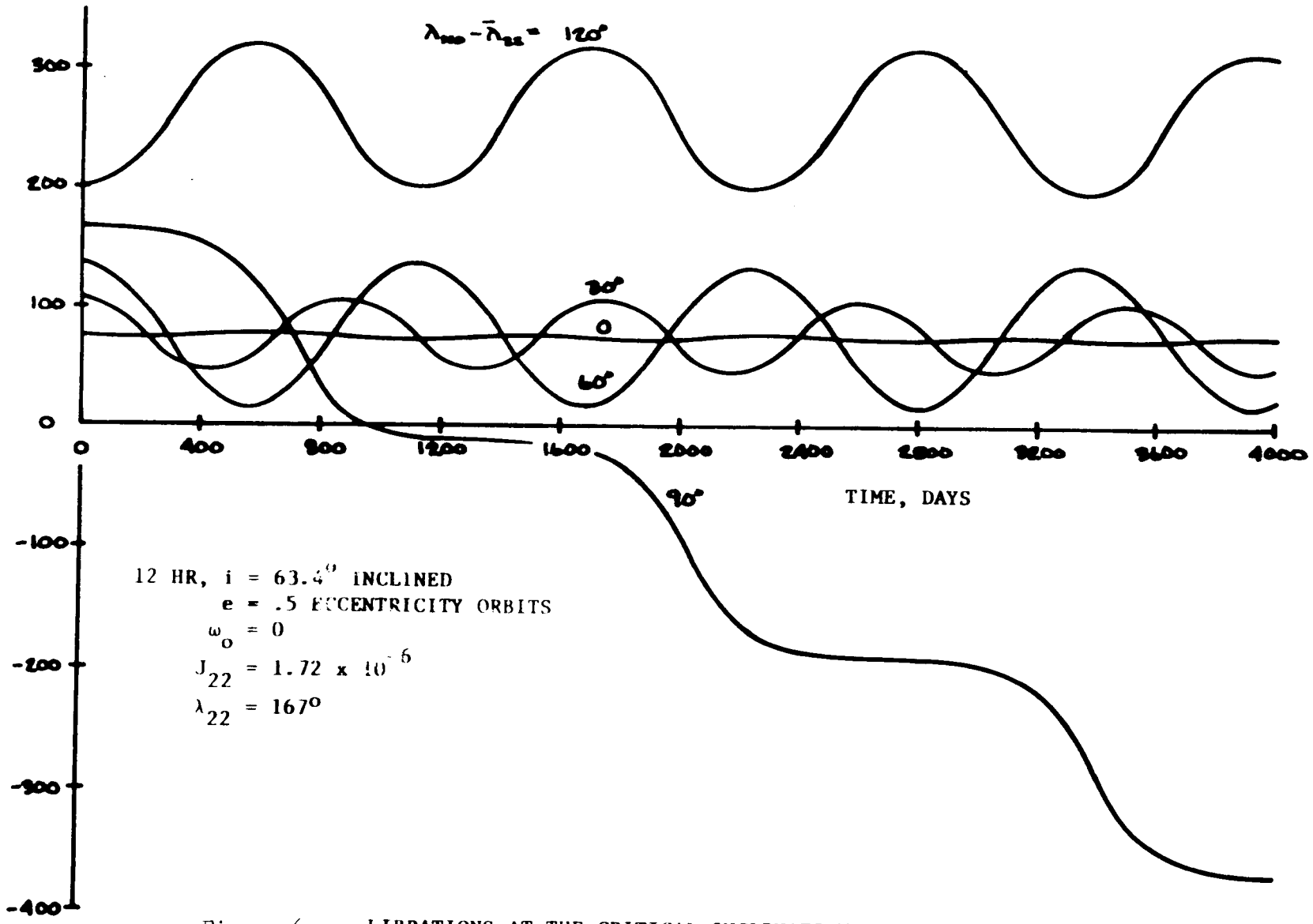

Figure 6. LIBRATIONS AT THE CRITICAL INCLINATION DUE TO V_{2211}

b) Initial Drift Rate, $\dot{\lambda}_{No} \neq 0$

If the semi-major axis of the orbit is not such that Equation (5) yields $\Delta s = 0$, the orbit is not strictly commensurate. As long as $\Delta s << 1$ resonance is effective, producing either libration or circulation.

To illustrate the effects of near, as opposed to exact, commensurability, a 12 hour 30 degree inclined circular orbit was chosen. Because the orbit is circular, we can restrict it to $q = 0$, and the critical term for a planetary observer is stationary. Figure 7 shows the calculated libration periods and amplitudes as functions of $(\lambda_{No} - \bar{\lambda}_{32})$ for zero initial drift velocity, i.e., for strictly commensurate orbits, and for a 30°/year initial drift rate. It can be seen that in the region $\pm$ 60 degrees around the stable node the orbits in the second case still librate. The effect of the initial drift rate is an increased amplitude which is already 30 degrees at the stable node. In the $\pm$ 30 degrees neighborhood of the unstable node the motion of λ_N becomes that of a pendulum turning over, and λ_N circulates producing a drift rate. Figure 8 is calculated for 60°/year initial drift rate which is enough to turn over the pendulum from everywhere except within $\pm$ 4 degrees of the stable node, and for 90°/year initial drift rate for which λ_N circulates for any initial position.

Figure 9 presents machine run results for 12 hour 30 degree inclined $e = 0.5$ eccentricity orbits with V_{220-1} alone. Since $q\dot{\omega} = 0$ the critical tesseral is rotating producing a -30°/year drift rate for strictly commensurate orbits also. As long as the $\bar{\dot{\lambda}}_{No} = \dot{\lambda}_{No} + 1/2\ \dot{\omega}$ does not carry λ_N over the "hump" the drift rate remains the same. Note that the $\dot{\lambda}_{No} = -69.35$ drifts with $-1/2\ \dot{\omega}$ but the $\dot{\lambda}_{No} = +69.35$ produces circulation and its drift rate is not -30° but 70°/year. With increasing initial drift rate the irregularity decreases and resonance becomes less and less pronounced. See Reference 16 for the case when the first term in Equation (11) becomes dominant.

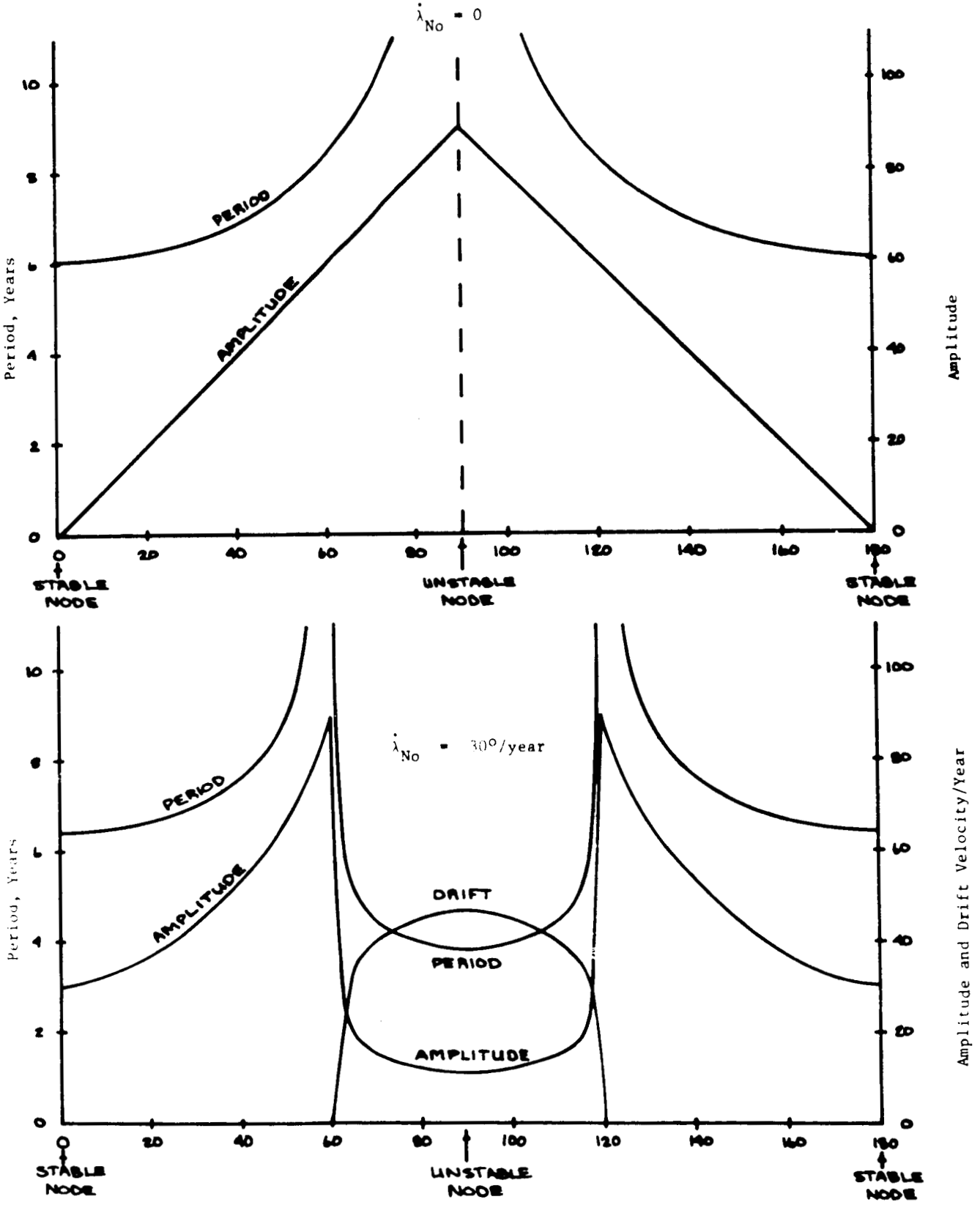

Figure 7. THEORETICAL VALUES OF AMPLITUDES, PERIODS, AND DRIFT VELOCITIES OF 12 HR., 30° INCLINED CIRCULAR ORBITS DUE TO V_{3210}.

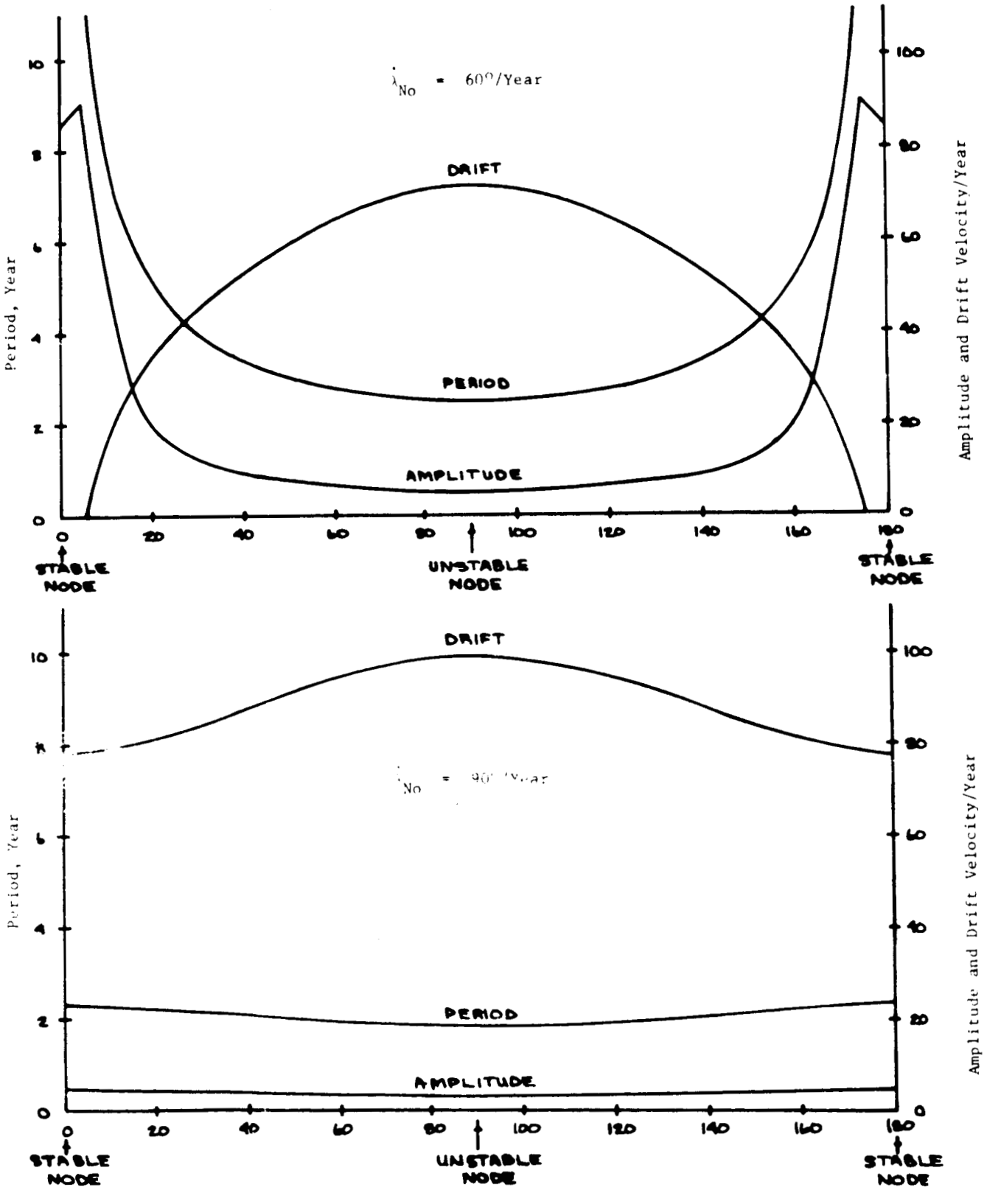

Figure 8. THEORETICAL VALUES OF AMPLITUDES, PERIODS, AND DRIFT VELOCITIES OF 12 HR., 30° INCLINED CIRCULAR ORBITS DUE TO V_{3210}.

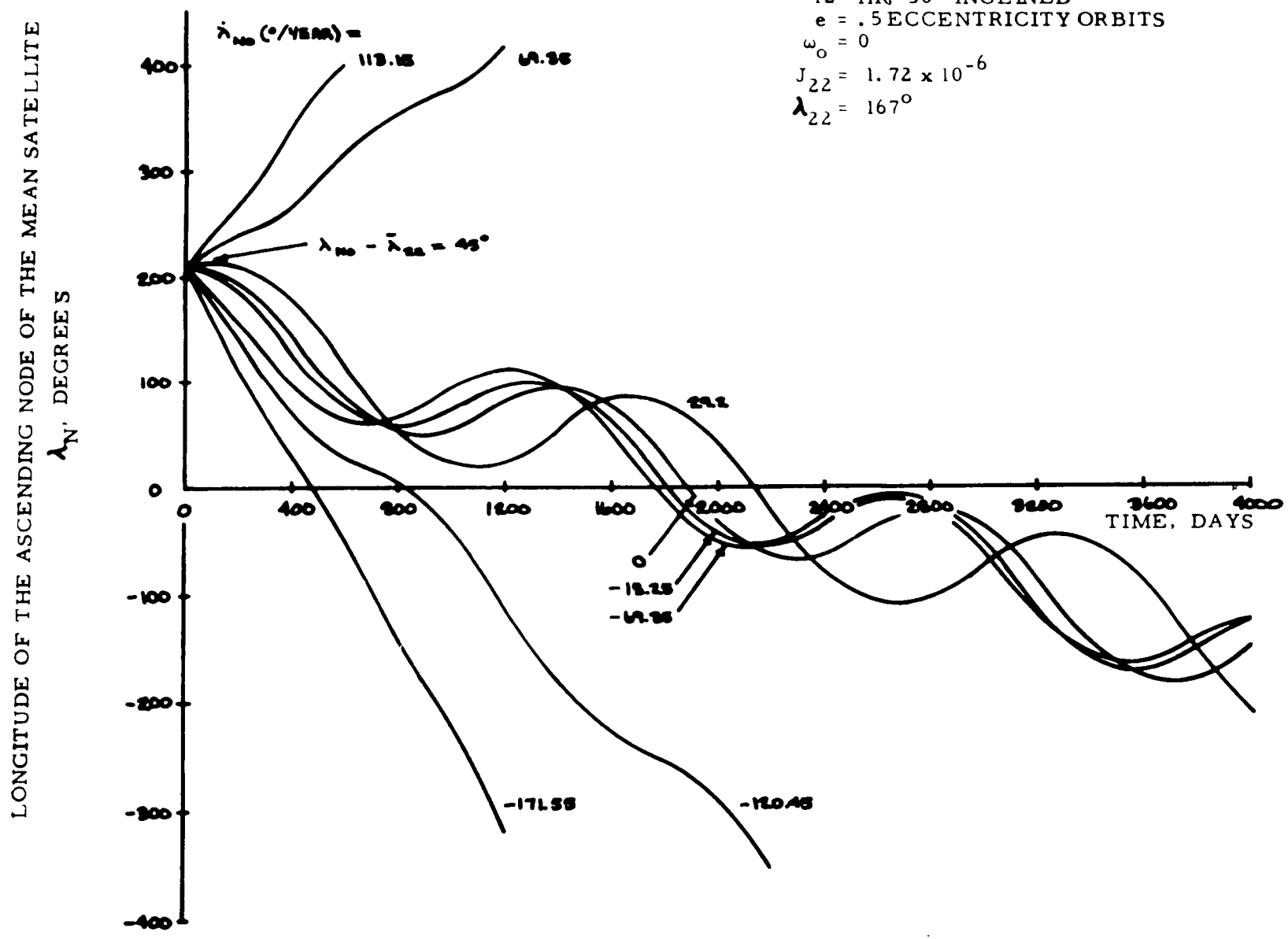

Figure 9. LIBRATIONS DUE TO V_{220-1}

5. THE GENERAL SOLUTION

In Section 2 a solution was presented when Equation (20) contains a single term. In the "real world" there are always several critical tesseral harmonics which enter into Equation (20); and, in general, no analytic solution is available. In some cases, however, good approximations can be obtained by neglecting certain less important terms. These are the low eccentricity and near equatorial orbits. The low eccentricity orbits were treated thoroughly in Reference 9, where it was shown that one of the harmonics will dominate the motion. For near equatorial orbits again one tesseral will dominate the motion because the inclination function is zero except for $(\ell - m)$ even and $p = \frac{1}{2}(\ell - m)$, which eliminates a number of critical terms.

For the "critical" inclination Equation (20) becomes autonomous. This allows an analytic solution.

Equation (20) can be written in the following form

$$\ddot{\lambda}_N = \frac{(2\pi)^2}{js_o} \sum_{\ell,q} \frac{1}{p^2_{\ell,q}} \sin [js_o\lambda_N - js_o\bar{\lambda}_{\ell m}] \tag{46}$$

with $j = 1, 2, \ldots$ and $\ell \geq js_o$.

In this equation cognizance was taken of the fact that m must be an integral multiple of s_o and that the value of p is defined by Equation (7) as soon as a pair of ℓ and q is selected. Equation (46) is still not solvable because of the different frequencies represented by the j values. Fortunately, the main frequency $j = 1$ dominates the motion due to the rapid decrease of field strength with ℓ. Thus a very good approximation can be found by neglecting the $j > 1$ values. Expanding Equation (46) the following is obtained

$$\ddot{\lambda}_N = -\frac{(2\pi)^2}{s_o} \sum_{\ell,q} \frac{1}{p^2_{\ell q}} [\sin s_o\lambda_N \cos s_o \bar{\lambda}_{\ell m} \cos s_o\lambda_N \sin s_o \bar{\lambda}_{\ell m}] \tag{47}$$

Introducing the phase angle ψ by

$$\tan s_o \psi = \frac{\sum_{\ell,q} \frac{1}{P_{\ell,q}^2} \sin s_o \bar{\lambda}_{\ell m}}{\sum_{\ell,q} \frac{1}{P_{\ell,q}^2} \cos s_o \bar{\lambda}_{\ell m}} \tag{48}$$

and the resultant period

$$P = \frac{1}{\left\{\left[\sum_{\ell,q} \frac{1}{P_{\ell,q}^2} \sin s_o \bar{\lambda}_{\ell m}\right]^2 + \left[\sum_{\ell,q} \frac{1}{P_{\ell,q}^2} \cos s_o \bar{\lambda}_{\ell m}\right]^2\right.} \tag{49}$$

with these Equation (47) becomes

$$\ddot{\lambda}_N = -s_o \left(\frac{2\pi/s_o}{P}\right)^2 \sin s_o (\lambda_N - \psi). \tag{50}$$

Again we have pendulum motion, with solution in the form of an elliptic integral of the first kind.

Figure 10 shows librations due to V_{220-1}, V_{2211}, and V_{3210} for a 12-hour orbit at the critical inclination, obtained by the RESORB program. Eccentricity was chosen maximum with the constraint that perigee be still drag-free. The curves shows pure libration and a stable node at 212 degrees, which agrees with the value calculated by Equation (47). It is interesting to note that this stable node falls in the midpoint between the stable nodes of V_{2211} and V_{3210} = 167 degrees and the stable node of V_{220-1} = 77 degrees + 180 degrees = 257 degrees.

For the rest of the cases the system is not autonomous and there are several critical tesserals which produce libration periods of equal order of magnitude. No analytic solution was found. Figure 11 showed examples obtained by the RESORB program for different initial conditions. Figure 12 shows the influence of mistargeting for only the two main components of J_{22}. The inclination and the initial node were selected such that the amplitude and the period should be the same for both terms. In spite of this precaution, the result is hardly predictable.

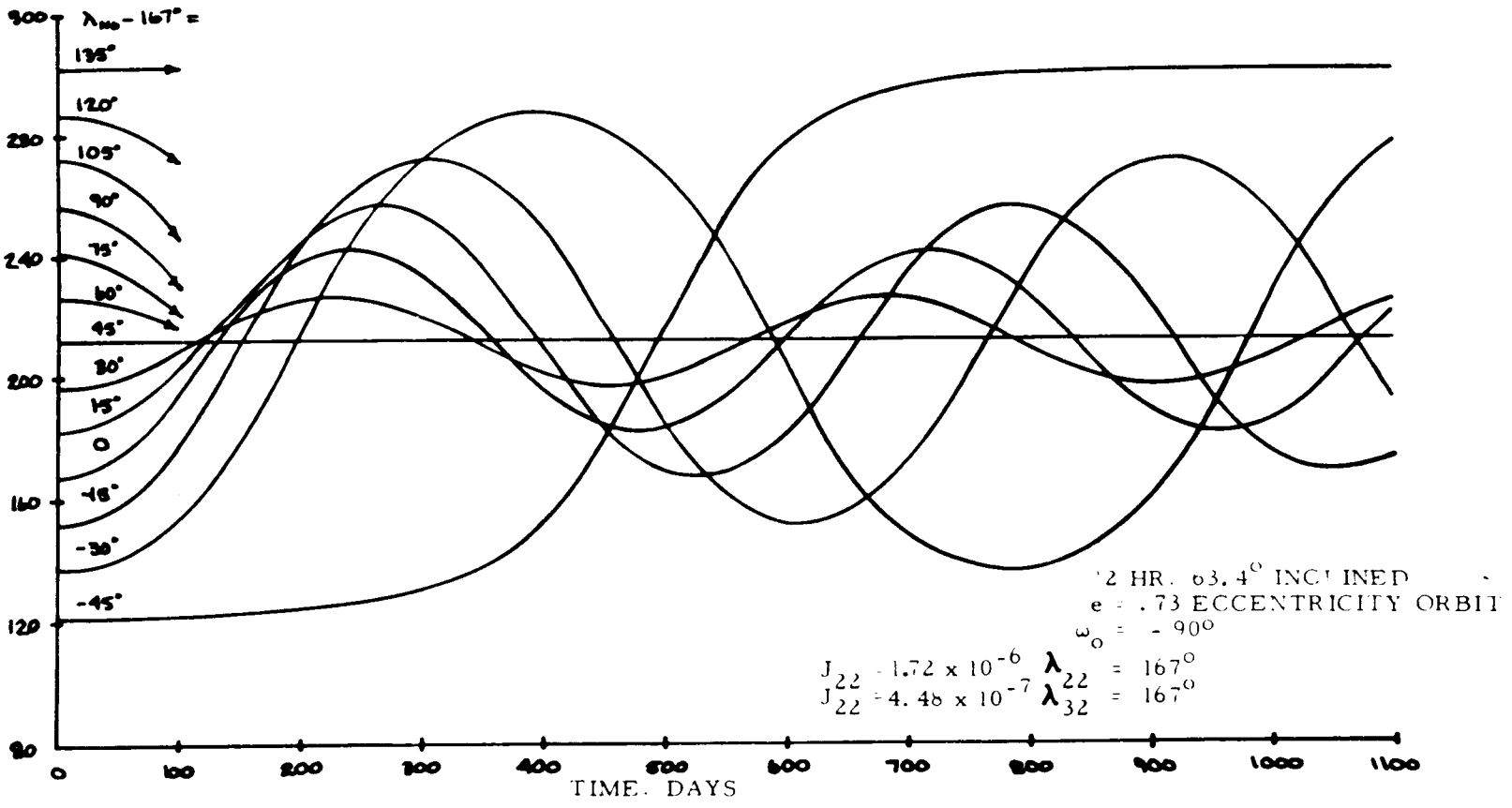

Figure 10 LIBRATIONS AT THE CRITICAL INCLINATION DUE TO V_{2211}, V_{220-1}, AND V_{3210}

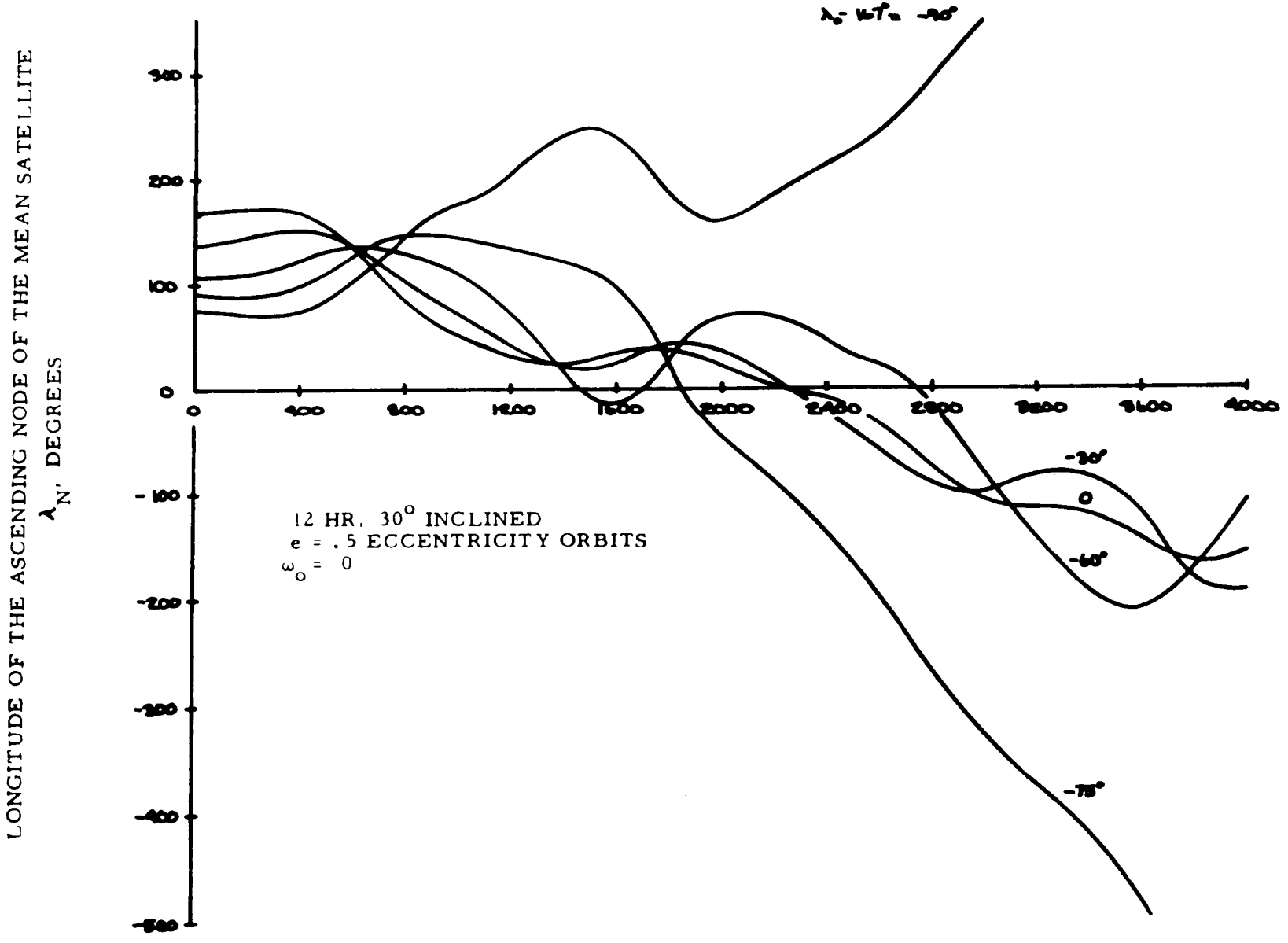

Figure 11 LIBRATION DUE TO ALL CRITICAL TESSERALS

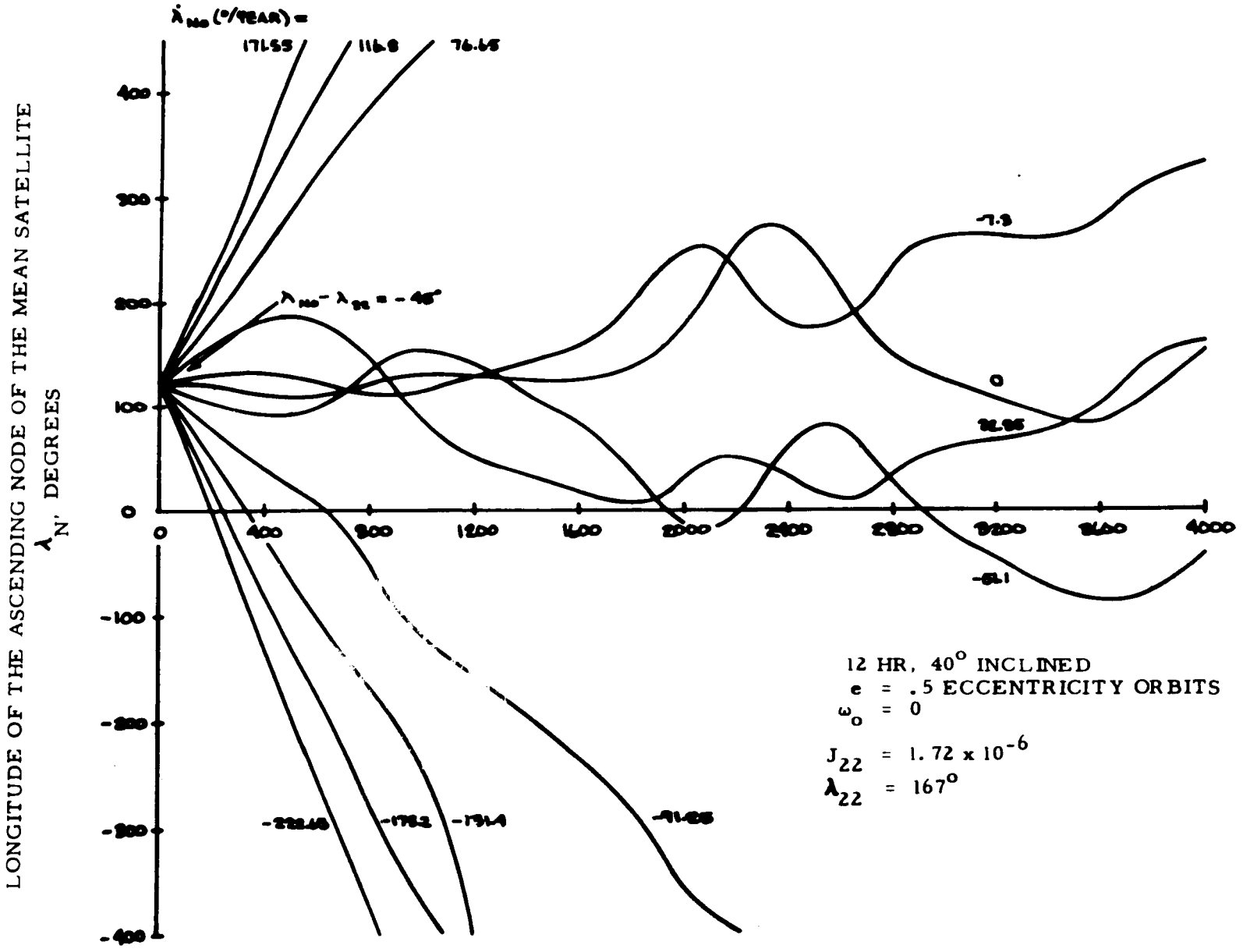

Figure 12. LIBRATIONS DUE TO V_{220-1} AND V_{2211}

REFERENCES

1. Morando, M. B., "Orbites de Resonance des Satellites de 24H," Bull. Astron. 24, 47 (1963).

2. Allan, R. R., "On the Motion of Nearly Synchronous Satellites," Royal Aircraft Establishment TR No. 64078 (1963).

3. Blitzer, L., "Effect of Ellipticity of the Equator on 24-Hour Nearly Circular Satellite Orbits," Journal of Geophys. Research, Vol. 67, No. 1 (1962).

4. Blitzer, L., "The Perturbed Motion of 24-Hour Satellites Due to Equatorial Ellipticity," Journal of Geophys. Research, Vol. 68, No. 3 (1963).

5. Blitzer, L., "Synchronous and Resonant Satellite Orbits Associated with Equatorial Ellipticity," ARS Journal 32, 1016 (1963).

6. Blitzer, L., "Equilibrium Positions and Stability of 24-Hour Satellite Orbits," Journal of Geophys. Research, Vol. 70, No. 16 (1965).

7. Blitzer, L., "Satellite Resonances and Librations Associated with Tesseral Harmonics of the Geopotential," Journal of Geophys. Research, Vol. 71, No. 11 (1966).

8. Garfinkel, Boris, "The Disturbing Function for an Artificial Satellite," Astron. J. Vol. 70, pp. 688-704 (1965).

9. Garfinkel, Boris, "Tesseral Harmonic Perturbations of an Artificial Satellite," Astron. J. Vol. 70, pp. 784 - 786 (1965).

10. Garfinkel, Boris, "Formal Solution in the Problem of Small Divisors," Astronomical J., 71 (8), pp. 657-669 (1966).

11. Wagner, C. A., "Longitudinal Variations of the Earth's Gravity Field as Sensed by the Drift of Three Synchronous Satellites," J. Geophys. Research, 71 (6), pp. 1703-1711 (1966).

12. Yionoulis, S. M., "A Study of the Resonance Effects Due to the Earth's Potential Function," J. Geophys. Research, 70 (24), pp. 5991-5996 (1965), 71 (4) (1966).

13. Francis, M. P., Gedeon, G. S., and Douglas, B. C., "Perturbations of Repeating Groundtrack Satellites by Tesseral Harmonics in the Gravitational Potential," AIAA Journal, Vol. 4, No. 7 (1966).

14. Anderle, R. J., "Observations of Resonance Effects on Satellite Orbits Arising from the Thirteenth- and Fourteenth-Order Tesseral Gravitational Coefficients," Journal of Geophysical Research, Vol. 70, No. 10 (1965).

REFERENCES (Continued)

15. Sheffield, Charles, "Linearized Solutions for a Circular Orbit Perturbed by Tesseral Harmonics," AIAA Journal, 4 (4), pp. 688-693 (1966).

16. Gedeon, G. S., and Dial, O. L., "Along-Track Oscillations of a Satellite Due to Tesseral Harmonics," AIAA Journal, Vol. 5, No. 3 (1967).

17. Kaula, W. M., Theory of Satellite Geodesy, Blaisdell Publishing Co., (1966).

18. Kaula, W. M., "Tests and Combination of Satellite Determinations of the Gravity Field with Gravimetry," JGR 71, 22, November 15, 1966.